In pursuit of the *ab initio* limit for conformational energy prototypes

Attila G. Császár
Department of Theoretical Chemistry, Eötvös University, H-1518 Budapest 112, P.O. Box 32, Hungary

Wesley D. Allen and Henry F. Schaefer III
Center for Computational Quantum Chemistry, Department of Chemistry, University of Georgia, Athens, Georgia 30602

(Received 23 December 1997; accepted 6 March 1998)

The convergence of *ab initio* predictions to the one- and n-particle limits has been systematically explored for several conformational energy prototypes: the inversion barriers of ammonia, water, and isocyanic acid, the torsional barrier of ethane, the E/Z rotamer separation of formic acid, and the barrier to linearity of silicon dicarbide. Explicit *ab initio* results were obtained with atomic-orbital basis sets as large as $[7s6p5d4f3g2h1i/6s5p4d3f2g1h]$ and electron correlation treatments as extensive as fifth-order Møller–Plesset perturbation theory (MP5), the full coupled-cluster method through triple excitations (CCSDT), and Brueckner doubles theory including perturbational corrections for both triple and quadruple excitations [BD(TQ)]. Subsequently, basis set and electron correlation extrapolation schemes were invoked to gauge any further variations in arriving at the *ab initio* limit. Physical effects which are tacitly neglected in most theoretical work have also been quantified by computations of non-Born–Oppenheimer (BODC), relativistic, and core correlation shifts of relative energies. Instructive conclusions are drawn for the pursuit of spectroscopic accuracy in theoretical conformational analyses, and precise predictions for the key energetic quantities of the molecular prototypes are advanced. © *1998 American Institute of Physics.* [S0021-9606(98)02422-2]

I. INTRODUCTION

In a seminal monograph of the 1960s, Eliel, Allinger, and co-workers[1] remark that, ''it is almost platitudinous to say that a chemist who does not understand conformational analysis does not understand organic chemistry. Even the area of physical chemistry related to molecular structure and physical properties has fallen heavily under the sway of conformational concepts.'' The years following this statement have witnessed a meteoric rise of the fields of molecular mechanics and *ab initio* quantum chemistry as a means of quantifying conformational considerations. The pinpoint determination of potential energy functions for large-amplitude molecular motion, as hindered by barriers of various types, remains a vexing problem for both theory and experiment, however. In the complexity of high-resolution far-infrared and Raman spectra lies an enormous wealth of information on the surfaces and dynamics of large-amplitude vibrations, provided the often insuperable inverse eigenvalue problem can be unravelled to some degree—whether at the minimal level of qualitative interpretation or in the extreme of rigorous quantum mechanical Hamiltonians applied to multidimensional potential energy functions. Methods of molecular quantum chemistry do not suffer from the inverse eigenvalue dilemma and thus provide both complementary and competitive approaches, but achieving accuracy for relative energies and conformational barriers to the level of about 1 cm^{-1} has heretofore been unreachable. The present investigation of conformational energy prototypes, including the NH_3, H_2O, and HNCO inversion barriers, the C_2H_6 torsional barrier, the HCOOH E/Z rotamer separation, and the SiC_2 barrier to linearity, conjoins the latest methods of electronic structure theory with recent advances in computer technology in a renewed pursuit of the complete accuracy inherent in the basis set and electron correlation limits of the quantum chemical armamentarium.

Among the best contemporary theoretical schemes for general thermochemical predictions is the Gaussian-2 approach and its modifications,[2] in which MP2, MP4, and QCISD(T) energies from basis sets up to $spdf$ in quality are employed with certain additivity approximations, and an empirical correction depending linearly on the number of paired/unpaired electrons is utilized to account for deviations from the *ab initio* limit. Another scheme for empirically based extrapolations toward this limit is the complete-basis-set (CBS) model of Petersson and co-workers.[3] The CBS model chemistries feature basis-set extrapolations based on formulas for the asymptotic convergence of pair natural orbital expansions, progressively higher order correlation treatments with basis sets of decreasing size, and empirical corrections for zero-point energy, spin contamination, and remaining correlation effects. Martin[4] has developed another empirical (three-parameter) energy correction scheme, which works for molecules having well-defined σ and π bonds and lone electron pairs. In addition, Siegbahn and co-workers[5] have proposed a simple parametrized configuration interaction (PCI-X) method which uses a single empirical scale factor to estimate *ab initio* limits from various correlation procedures with modest basis sets.

Recent advances have also been achieved in electronic structure methods which provide highly accurate thermochemistry without empirical parametrization. Indispensable

for such pursuits is an understanding of the asymptotic behavior of finite-order correlation energies with respect to basis-set augmentation, as examined in the helium-atom archetype by Schwartz[6] in 1962 and by Carroll *et al.*[7] in 1979. The analysis was extended by Kutzelnigg and Morgan[8] in 1992 to second- and third-order energies of all possible two-electron atoms and also to MP2 energies of arbitrary n-electron atoms; in particular, coefficients were derived for the leading terms in the $(l+1/2)^{-n}$ partial-wave expansion of the atomic correlation energy. Assuming saturation of the radial basis, the contribution to $E^{(2)}$ from angular momentum l decays asymptotically as $(l+1/2)^{-4}$ for natural parity singlet states, as $(l+1/2)^{-6}$ for triplet states, and as $(l+1/2)^{-8}$ for unnatural parity singlet states.

In molecular environments, systematic approach to one-particle limits is made possible by the correlation-consistent families of basis sets (cc-pVXZ, aug-cc-pVXZ, and cc-pCVXZ) developed by Dunning and co-workers.[9–12] Several energy extrapolation formulas have been proposed involving the cardinal number (X) in these series, which also represents the highest spherical harmonic contained in the basis set. The assumption that incremental ($X \rightarrow X+1$) lowerings of the total energy lie in a geometric progression is equivalent to extrapolation via the exponential form of Feller,[13] viz.,

$$E = E_\infty + a e^{-bX}. \tag{1}$$

While this form appears operative for Hartree–Fock energies, computational evidence indicates that it underestimates correlation energy limits.[14,15] The aforementioned partial-wave analyses suggest alternatives, but they rigorously apply only to expansions in which the radial space is first saturated for each l, whereas the correlation-consistent basis sets are built up with radial and angular functions simultaneously to achieve an energy lowering balance. With due caution for identifying X with l, Helgaker, Klopper, Koch, and Noga[14] have proposed a simple, *integrated* Schwartz expression for extrapolation of correlation energies,

$$E = E_\infty + \frac{b}{X^3}, \tag{2}$$

while Martin[15] has chosen a phenomenological inverse-power form for first-row species,

$$E = E_\infty + \frac{a}{(X+1/2)^4} + \frac{b}{(X+1/2)^6}, \tag{3}$$

termed Schwartz4 ($b=0$) or Schwartz6 ($b\neq 0$).

Schemes for performing n-particle extrapolations to the full configuration interaction limit also abound. Most pertinent here are two formulas[16,17] for the total basis-set correlation energy ($\varepsilon_{\rm corr}$) involving the nth-order terms (ε_n) of the Møller–Plesset (MP) perturbation series

$$\varepsilon_{\rm corr} = \frac{\varepsilon_2+\varepsilon_3}{1-\varepsilon_4/\varepsilon_2}, \tag{4}$$

and the shifted [2,1] Padé approximant

$$\varepsilon_{\rm corr} = \frac{\varepsilon_2^2(\varepsilon_4-\varepsilon_5)+2\varepsilon_2\varepsilon_3(\varepsilon_4-\varepsilon_3)+\varepsilon_3^2(\varepsilon_2-\varepsilon_3)}{(\varepsilon_2-\varepsilon_3)(\varepsilon_4-\varepsilon_5)-(\varepsilon_4-\varepsilon_3)^2}, \tag{5}$$

which is based on the rational extrapolation

$$\varepsilon_2+\lambda\varepsilon_3+\lambda^2\varepsilon_4+\lambda^3\varepsilon_5+\cdots \approx \frac{a_0+a_1\lambda}{1+b_1\lambda+b_2\lambda^2}. \tag{6}$$

Both schemes have been subjected to limited testing.[18–20] The first formula only requires energies through fourth order, but in our experience it frequently underestimates higher-order contributions to relative energies. If fifth-order energies can be obtained, Eq. (5) appears to be a much better estimator of the full CI limit, albeit less accurate than schemes which include both sixth-order energies and different formulas for monotonic vs. oscillatory series.[20] Of course, the alternative concept of combining explicit CI computations with perturbation theory by means of a variable threshold for configuration selection is well established.[21–24] The efficacious convergence/extrapolation to the full configuration interaction limit via a series of CI-PT computations of diminishing threshold has been amply demonstrated in several recent studies.[13,25–27] Finally, the most theoretically sound approach to pinpointing *ab initio* limits is probably provided by R12[28] or Gaussian geminal[29,30] methods, which effectively deal with the electron–electron cusp problem by employing wave functions depending explicitly on interelectronic distances.

In the present research, the dual extrapolation of relative energy predictions to the one- and n-particle *ab initio* limits is performed within the focal-point scheme of Allen and co-workers,[31–35] whose characteristics generally include: (a) use of a family of basis sets which systematically approaches completeness (e.g., the cc-pVXZ, aug-cc-pVXZ, and cc-pCVXZ sets); (b) application of low levels of theory with prodigious basis sets (typically direct RHF and MP2 computations with several hundred basis functions); (c) higher-order valence correlation treatments [CCSDT, CCSD(T), BD(TQ), MP4, and MP5] with the largest possible basis sets; (d) layout of a two-dimensional extrapolation grid based on an assumed additivity of correlation *increments* to the energy difference of concern; and (e) eschewal of empirical corrections. Previous focal-point work[32] and numerous other theoretical studies have shown that even in systems without particularly heavy atoms, account may also be needed for core correlation[32,36–39] and relativistic phenomena,[40–44] as well as the Born–Oppenheimer diagonal correction (BODC).[45,46] Therefore, auxiliary shifts for these effects have been appended here to valence focal-point analyses not only to ensure the highest possible accuracy but also to enhance our understanding of their manifestations for conformational energy prototypes.

II. COMPUTATIONAL METHODS

Because the (aug)-cc-p(C)VXZ correlation-consistent families of basis sets[9–12] approach completeness in a very systematic fashion, they were employed in the focal-point extrapolations of the present study. Specifically, the cc-pVXZ ($X=2-6$), aug-cc-pVXZ ($X=3-5$), and cc-pCVXZ ($X=2-4$) basis sets were utilized, whose contracted Gaussian orbitals for the [(C,N,O)/H] atoms range as $[3s2p1d/2s1p] \rightarrow [7s6p5d4f3g2h1i/6s5p4d3f2g1h]$,

$[5s4p3d2f/4s3p2d] \rightarrow [7s6p5d4f3g2h/6s5p4d3f2g]$, and $[4s3p1d/2s1p] \rightarrow [8s7p5d3f1g/4s3p2d1f]$, respectively. In the (aug) extension of each cc-pVXZ basis, diffuse $[1s1p1d...1Y_X/1s1p...1Y_{X-1}]$ sets, involving spherical harmonics (Y_l) with angular momentum quantum numbers as large as $l=X$, are appended for the description of molecular properties and spatially extended charge distributions, whereas the corresponding (C) augmentation includes tight $[(X-1)s,\ (X-1)p,\ (X-2)d,\ ...2Y_{X-2},\ 1Y_{X-1}]$ sets for the heavy atoms with polarization functions through $l=X-1$ for the recovery of core correlation. In selected cases, a hybrid set denoted cc-pVTZ/DZ and constructed as [cc-pVTZ/cc-pVDZ] for [(C,N,O)/H] was employed to decrease the size of the molecular one-particle basis in higher-order correlation treatments. The effect of this compromise on relative energies was found to be insignificant. Several extrapolation schemes were investigated for the estimation of total energies at the complete basis set limit, but the final predictions involved the fitting of ($X=4,\ 5,\ 6$) sets of cc-pVXZ RHF and MP2 energies to the functional forms of Eqs. (1) and (2), respectively.

Reference electronic wave functions were generally determined by the single-configuration restricted Hartree–Fock (RHF) method.[47,48] Dynamical electron correlation was accounted for by Møller–Plesset perturbation theory from second through fifth order (MP2–MP5),[48–50] or by the coupled-cluster (CC) method[51] including all single and double (CCSD)[51,52] and in cases triple excitations (CCSDT).[53] For all molecules the CCSD(T) method,[54] which includes a perturbative term [(T)] for connected triple excitations, was also employed. Finally, for the HNCO molecule, agreement with extrapolated MPn results was improved by extending the coupled-cluster approach past the (T) augmentation, as provided by the Brueckner doubles (BD) method[55] with perturbational estimates for both connected triple and quadruple excitations [BD(TQ)].[50] For valence focal-point correlation energy computations, the 1s core orbitals of the carbon, nitrogen, and oxygen atoms were excluded from the active space, while no virtual orbitals were frozen. Core correlation effects were then determined by means of all-electron treatments with the cc-pCVXZ basis sets. Extrapolation of the MPn series[17–20] was performed via shifted [2,1] Padé approximants [Eq. (5)] when fifth-order energies were available. The program packages PSI,[56] GAUSSIAN94,[57] and ACESII[58] were used for the electronic structure computations.

Analytic gradient techniques[59] were utilized to obtain optimum geometric structures at the cc-pVTZ or aug-cc-pVTZ unfrozen-core CCSD(T) level of theory, as specified in the footnotes of the data tables to follow. These structures were adopted for all electronic computations involved in the valence focal-point analyses and the auxiliary BODC, relativistic, and core correlation corrections. Comparison of the reference theoretical structures with available empirical r_e and r_m^{ρ} parameters for NH_3,[60] H_2O,[61] HNCO,[62] C_2H_6,[61] and HCOOH[61] reveals average discrepancies of only 0.002 Å and 0.08° for the bond distances and angles, excluding the questionable case of r(C–H) for formic acid.

Relativistic effects were gauged by first-order perturbation theory applied to the one-electron mass-velocity and Darwin terms,[40] as implemented for Hartree–Fock and correlated wave functions within the ACESII program system.[44,58] Computation of the Born–Oppenheimer diagonal correction (BODC) for potential energy surfaces was performed at the Hartree–Fock level within the formalism of Handy, Yamaguchi, and Schaefer[45] and by means of the BORN program operating within the PSI package.[56]

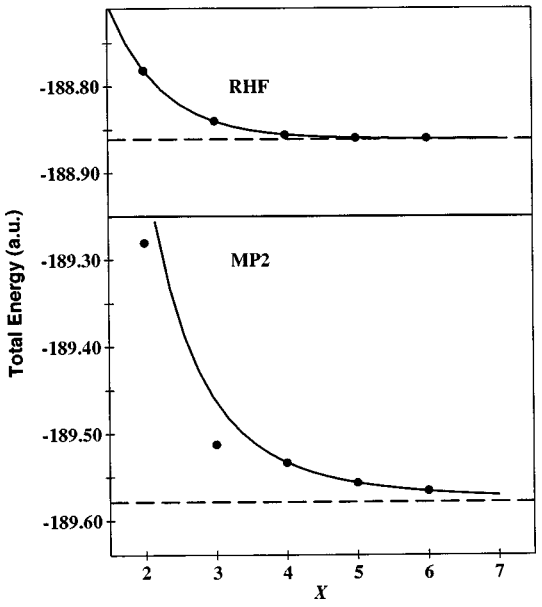

FIG. 1. The cc-pVXZ series of RHF and MP2 total energies for the Z conformer of formic acid determined at the unfrozen-core cc-pVTZ CCSD(T) optimum structure (Table V, footnote a). The solid lines result from fits of the ($X=2-6$) RHF total energies and the ($X=4-6$) MP2 correlation energies to Eqs. (1) and (2) of the text, respectively.

III. RESULTS AND DISCUSSION

The valence focal-point analyses for the inversion barriers in NH_3, H_2O, and HNCO, the torsional barrier in C_2H_6, and the E/Z isomerization energy in HCOOH are presented in Tables I–V, in order. The absolute total energies from which the relative energies derive are too extensive to be listed here but may be obtained from the authors upon request. Figure 1 is a representative plot of ($X=2-6$) cc-pVXZ RHF and MP2 total energies, as computed for the lowest-energy (Z) conformer of formic acid. Auxiliary non-Born–Oppenheimer (BODC), relativistic, and core correlation shifts for the conformational energy prototypes are collected in Table VI. The results in these tables push the *ab initio* envelope well beyond the usual criterion for chemical accuracy (1 kcal mol^{-1}) and provide lessons in the pursuit of spectroscopic accuracy (1 cm^{-1}) by traditional electronic structure methods.

A. The inversion barrier of ammonia

Myriad empirical and theoretical studies[32,39,63–78] have addressed the inversion barrier associated with the ν_2 umbrella mode in ammonia. The earliest experimental attempts employed models where no or limited interaction was permitted between the inversion motion and complementary vibrations. In subsequent work the model potential energy sur-

TABLE I. Valence focal-point analysis of the inversion barrier (ΔE_e, cm^{-1}) of ammonia.[a,b]

		Series 1					Series 2			
	ΔE_e(RHF)	δ[MP2]	δ[MP3]	δ[MP4]	δ[MP5]	δ[MP∞]	ΔE_e(MP∞)	δ[CCSD]	δ[CCSD(T)]	δ[CCSDT]	ΔE_e(CCSDT)
cc-pVDZ (29)[c]	**2505**	+285	+61	+121	−6	+4	**2970**	+101	+85	+5	**2981**
cc-pCVDZ (33)	**2485**	+311	+56	+123	−9	+5	**2971**	+98	+84	+4	**2982**
cc-pVTZ (72)[c]	**1852**	+220	+32	+130	−30	+14	**2218**	+88	+65	+1	**2226**
cc-pCVTZ (85)	**1861**	+219	+32	+133	−32	+14	**2227**	+89	+66	+2	**2237**
aug-cc-pVTZ (115)	**1647**	+121	+64	+108	[−30]	[+14]	**[1924]**	+129	+38	+2	**1937**
cc-pVQZ (145)	**1737**	+141	+27	+130	[−30]	[+14]	**[2019]**	+92	+53	[+2]	**[2025]**
cc-pCVQZ (174)	**1737**	+138	+28	+130	[−30]	[+14]	**[2017]**	+93	+53	[+2]	**[2023]**
aug-cc-pVQZ (218)	**1629**	+78	+55	+112	[−30]	[+14]	**[1858]**	+121	+39	[+2]	**[1869]**
cc-pV5Z (256)	**1649**	+86	+46	+123	[−30]	[+14]	**[1888]**	[+121]	[+39]	[+2]	**[1897]**
aug-cc-pV5Z (367)	**1627**	+55	[+46]	[+123]	[−30]	[+14]	**[1835]**	[+121]	[+39]	[+2]	**[1844]**
cc-pV6Z (413)	**1632**	+57	[+46]	[+123]	[−30]	[+14]	**[1842]**	[+121]	[+39]	[+2]	**[1851]**
Extrapolation limit (∞)[d]	**1628**	+24	[+46]	[+123]	[−30]	[+14]	**[1805]**	[+121]	[+39]	[+2]	**[1814]**

[a]The symbol δ denotes the *increment* in the relative energy (ΔE_e) with respect to the preceding level of theory, as given by the competing higher-order correlation series 1 [RHF→MP2→MP3→MP4→MP5→MP∞] and series 2 [RHF→MP2→CCSD→CCSD(T)→CCSDT]. The higher-order correlation increments listed in brackets are taken for the purpose of extrapolation from corresponding entries for smaller basis sets, thus yielding the net ΔE_e values also appearing in brackets. For each basis set the total number of contracted Gaussian functions is given in parentheses.

[b]All total energies were computed at unfrozen-core aug-cc-pVTZ CCSD(T) optimized geometries: r(N–H) = 1.011 98 (0.995 19) Å and ∠(H–N–H) = 106.686 (120.0)° in the $C_{3v}(D_{3h})$ cases.

[c]The corresponding cc-pVXZ{RHF, δ[MP2], δ[CCSD], δ[CCSD(T)]}//cc-pVXZ CCSD(T) data are {2396, 480, 114, 113} and {1828, 250, 88, 69} cm^{-1}, respectively, in the $X=D$ and T cases.

[d]Based on $X=(4, 5, 6)$ cc-pVXZ RHF and MP2 total energies fit, respectively, to Eqs. (1) and (2) of the text.

faces and rovibrational quantum mechanical treatments became increasingly sophisticated. In a fully variational calculation of the lower vibrational energy levels, based on a six-dimensional, simple potential and the Watson Hamiltonian, Maessen *et al.*[66] arrived at a bare inversion barrier of 1810 cm^{-1} by a fit to available spectroscopic data. Spirko and co-workers[68] have empirically determined the inversion barrier of NH_3 from multiparameter potential fits of observed $(\nu_1, \nu_2^{\pm}, \nu_3^l, \nu_4^l) = (\{0,1\}, \{0^{\pm}, 1^{\pm}, 2^{\pm}, 3^{\pm}, 4^{\pm}\}, \{0^0, 1^1, 2^2\}, \{0^0, 1^1, 2^0, 2^2\})$ vibrational levels to a nonrigid invertor Hamiltonian. These and earlier[63] procedures predict *effective* one-dimensional, vibrationally averaged barriers in the 2018 ± 10 cm^{-1} range. The empirical analyses have differed widely regarding the zero-point vibrational energy (ZPVE) effect, inferring bare classical inversion barriers scattered from 1794 to 1885 cm^{-1}.[68] *Ab initio* work[32] suggests that the magnitude of the ZPVE correction is even larger. For the pyramidal form, DZP CISDTQ harmonic vibrational frequencies[74] yield a complementary-mode ZPVE which is only 3.7% larger than the anharmonic result given by the highly accurate cc-pVQZ CCSD(T) complete quartic force field of Martin, Lee, and Taylor.[78] The same DZP CISDTQ frequencies for planar ammonia, when scaled downward by 3.7% for anharmonic effects and residual errors, predict a ZPVE correction of −244 cm^{-1} for the inversion barrier, which is adopted for the present work.

The early DZP CISD computations of Bunker and co-workers[73] gave a barrier height of 1995 cm^{-1}, in broad agreement with the then available spectroscopic data. It became clear quite early[70,73] that the electron correlation contribution to the barrier is positive, its value being put around +120 cm^{-1}, but basis-set effects have persistently been underestimated. Although the QZ2P RHF calculations of Rodwell and Radom[72] were considered[73] to be of near-Hartree–Fock quality, present data (*vide infra*) indicate that the resulting barrier height of 1822 cm^{-1} is almost 200 cm^{-1} above the HF limit. Perhaps the best current *ab initio* predictions of the inversion barrier of ammonia, based on extensive computations with a variety of basis sets up to aug-cc-pVQZ in quality and correlation treatments as extensive as CCSD(T), are those of Allen, East, and Császár,[32] and East and Radom.[39] The latter investigation arrived at a classical barrier of 1821 cm^{-1}. Despite all of these studies, the first-principles characterization of the inversion mode of ammonia still attracts considerable interest.[77]

The present focal-point analysis of the inversion problem for ammonia (Table I) begins with the cc-pVDZ basis, which yields quite severe overestimations of the barrier. The cc-pVDZ RHF value of 2505 cm^{-1} is increased to 2790 cm^{-1} by second-order perturbation theory and then to 2972 cm^{-1} in fourth order before correlation convergence is observed. Both the cc-pVDZ MP∞ and CCSDT barriers are ca. 1000 cm^{-1} too large as a consequence of basis set deficiences, which are more severe for the diffuse lone electron pair in the planar structure. As the one-particle basis is enlarged, the ΔE_e(RHF) and ΔE_e(MP2) values exhibit a conspicuous and steady decrease over ranges of 900 and 1100 cm^{-1}, respectively. The persistent reduction of the δ[MP2] increment from approximately +300 cm^{-1} to just over +50 cm^{-1} is striking. Augmentation of the cc-pVXZ basis sets provides much more rapid convergence of the RHF and MP2 barrier predictions; *n.b.*, corresponding aug-cc-pVXZ and cc-pV$(X+1)$Z results are in close agreement. Nonetheless, the variations in Table I demonstrate that the inversion barrier of ammonia is not predicted to within 50 cm^{-1} until the aug-cc-pV5Z or cc-pV6Z basis set is employed!

Contrary to the one-particle convergence behavior, the

competing electron correlation series for the inversion barrier of ammonia approach limiting values relatively rapidly. The net MP2→MP4 and MP2→CCSD(T) barrier shifts are +162 and +153 cm^{-1}, respectively, in the representative cc-pVTZ case. In accord with the assumptions of the focal-point scheme, the basis set dependence of such higher-order correlation increments is modest, as exemplified by cc-pVTZ→cc-pV5Z variations in δ[MP3] and δ[MP4] of less than 20 and 10 cm^{-1}, in order. The highest-order cc-pVTZ (δ[MP5], δ[MP∞], δ[CCSDT]) set of contributions is only (−30, +14, +1) cm^{-1}, and the corresponding CCSDT and extrapolated MP∞ barriers differ by only 8 cm^{-1}. Moreover, the valence focal-point results for series 1 and 2 agree within 9 cm^{-1} for all basis sets larger than aug-cc-pVTZ, suggesting their propinquity to the full-CI limit. Such comforting agreement is indeed consistent with earlier observations[32] that the DZP CCSD(T) barrier differs from the complete DZP CISDTQ prediction[74] by a mere 1 cm^{-1}.

The cc-pVXZ and aug-cc-pVXZ sequencies of Hartree–Fock total energies and second-order correlation energies were subjected to various extrapolation procedures to obtain ∞ RHF and ∞ MP2 estimates. The exponential form of Eq. (1) appears operative in the RHF series, and its application to the cc-pVXZ (X=4, 5, 6) data predicts the (C_{3v},D_{3h}) Hartree–Fock limiting values (−56.224 95, −56.217 54) E_h, or 1628 cm^{-1} for the barrier. However, the falloff of the MP2 correlation energies is indeed much slower than exponential (*vide supra*), prompting alternative fits of the cc-pVXZ or aug-cc-pVXZ data not only to Eq. (2) but also to the SchwartzK(lmn) and aug-SchwartzK(lmn) variants of Martin.[15] Such exploratory fits, supplemented by sensitivity tests for the exclusion of individual points, indicate that the valence second-order correlation energy cannot be extrapolated from X=5 or 6 to infinity with an accuracy better than about 0.4 mE_h and that an uncertainty of ±20 cm^{-1} becomes inherent in the estimated δ[MP2] limits for the barrier. The rms error for the fit of the cc-pVXZ (X=4, 5, 6) data to Eq. (2) is an order of magnitude better than in the aug-cc-pVXZ (X=3, 4, 5) case, and the cc-pVXZ δ[MP2] limit derived therefrom (+24 cm^{-1}) is intermediate among the sundry extrapolation estimates. Hence, the +24 cm^{-1} ∞MP2 increment has been adopted for the final focal-point extrapolation in Table I, which yields vibrationless barriers for series 1 and 2 of 1805 and 1814 cm^{-1}, respectively.

Because the inversion of ammonia entails sp rehybridization at the nitrogen center and associated changes in core penetration effects and core–valence interactions, both the relativistic and core correlation shifts of the barrier (Table VI) are non-negligible at the level of precision sought in this study. The relativistic shift is just under +23 cm^{-1}, varying only 0.1 cm^{-1} among the cc-pVTZ RHF, MP2, and CCSD results. The core correlation effect is substantially larger and acts in the opposite direction. The cc-pCVTZ MP2, CCSD, and CCSD(T) predictions all lie between −53 and −56 cm^{-1}, suggesting that second-order perturbation theory is sufficient for recovering core correlation effects on *relative* energies along the inversion path. Accordingly, we adopt a final prediction of −64 cm^{-1}, as given by the MP2 method with the larger cc-pCVQZ basis set. The BODC correction (−10.7 cm^{-1}) provides a slight augmentation to this shift.

The final theoretical value for the classical inversion barrier of ammonia is obtained by adding the average valence focal-point result to the auxiliary corrections: ΔE_e=1810 +23−64−11=1758 cm^{-1} (5.026 kcal mol^{-1}). Among the scattered empirical inversion barrier heights, the set of *effective* one-dimensional spectroscopic results in the 2018±10 cm^{-1} interval[63,68] now exhibits the best agreement with theory, provided the aforementioned *ab initio* correction of −244 cm^{-1} is adopted for zero-point vibrations to shift the range to 1774±10 cm^{-1}. With the theoretical improvements achieved here for the classical barrier, any further resolution of the inversion problem in ammonia should await an explicit high-level *ab initio* treatment of the anharmonicity of the complementary modes of vibration in the pyramidal vs the planar structure.

B. The inversion barrier of water

Due to the special role the water molecule plays in the physics and chemistry of the atmospheres of planets and stars,[79] of the interstellar medium, and of combustion systems, an enormous number of experimental and theoretical studies[14,79–95] have explored the ground-state potential energy surface of free water. A salient aspect of the surface is the barrier to linearity. Although this inversion barrier is about six times larger than that of ammonia, its effect on the excited-state vibrational dynamics of the bending mode has been observed repeatedly in computations by both perturbational[80–82] and variational[85,86] techniques. Even in variational approaches, a breakdown occurs after more than 4 quanta appear in the bending mode if the chosen analytic form of the potential does not have the correct behavior at linearity. Increased spectroscopic capabilities for the detection of higher-lying bending states[87,88] bring the precise determination of the inversion barrier within reach. Nonetheless, few of the detailed *ab initio* studies of water[14,76,81,89–95] have addressed the barrier to linearity of this prototype, prompting the current focal-point analysis in Table II.

As observed for ammonia, extension of the one-particle basis set systematically lowers the inversion barrier to apparent convergence, and augmentation with diffuse functions provides a critical improvement which makes analogous aug-cc-pVXZ and cc-pV(X+1)Z results comparable. As a particular case, the cc-pVQZ overestimation of the extrapolated RHF barrier (11 246 cm^{-1}) is 104 cm^{-1}, whereas both the aug-cc-pVQZ and cc-pV5Z RHF results lie within 8 cm^{-1} of this inferred limit. The δ[MP2] increment exhibits dramatic changes over the basis set series, transforming steadily from a large positive value (+352 cm^{-1}) with the small cc-pVDZ basis to a large negative value (−305 cm^{-1}) in the cc-pV6Z case. As demonstrated by the cc-pV5Z→cc-pV6Z change in δ[MP2] of 48 cm^{-1}, clear convergence of the first correlation increment to the barrier is not observed even after extension of the basis through [7s6p5d4f3g2h1i/6s5p4d3f2g1h] quality.

The higher-order electron correlation contributions to the water barrier are small, and notwithstanding the torpid convergence at the MP2 level, they are relatively insensitive to

TABLE II. Valence focal-point analysis of the inversion barrier (ΔE_e, cm^{-1}) of water.[a]

		Series 1					Series 2			
	ΔE_e(RHF)	δ[MP2]	δ[MP3]	δ[MP4]	δ[MP5]	δ[MP∞]	ΔE_e(MP∞)	δ[CCSD]	δ[CCSD(T)]	δ[CCSDT]	ΔE_e(CCSDT)
cc-pVDZ (24)[b]	**12 206**	+352	+117	+155	−2	+5	**12 833**	+173	+94	+6	**12 831**
cc-pCVDZ (28)	**12 176**	+396	+114	+162	−7	+6	**12 837**	+165	+94	+5	**12 836**
cc-pVTZ (58)[b]	**11 519**	+102	+87	+180	−43	+18	**11 863**	+189	+54	+2	**11 866**
cc-pCVTZ (71)	**11 521**	+102	+89	+186	−49	+20	**11 870**	+193	+56	+2	**11 874**
aug-cc-pVTZ (92)	**11 280**	−144	+161	+79	+24	−1	**11 399**	+266	−11	+3	**11 394**
cc-pVQZ (115)	**11 350**	−128	+95	+151	[+24]	[−1]	**[11 491]**	+212	+17	+3	**11 454**
cc-pCVQZ (144)	**11 351**	−134	+97	+152	[+24]	[−1]	**[11 489]**	+214	+17	[+3]	**[11 451]**
aug-cc-pVQZ (172)	**11 254**	−267	+145	+86	[+24]	[−1]	**[11 241]**	+257	−15	[+3]	**[11 232]**
cc-pV5Z (201)	**11 248**	−257	+133	+114	[+24]	[−1]	**[11 261]**	+250	−5	[+3]	**[11 239]**
aug-cc-pV5Z (287)	**11 249**	−301	+149	+93	[+24]	[−1]	**[11 213]**	[+250]	[−5]	[+3]	**[11 196]**
cc-pV6Z (322)	**11 245**	−305	[+149]	[+93]	[+24]	[−1]	**[11 205]**	[+250]	[−5]	[+3]	**[11 188]**
Extrapolation limit (∞)[c]	**11 246**	−382	[+149]	[+93]	[+24]	[−1]	**[11 129]**	[+250]	[−5]	[+3]	**[11 112]**

[a]All total energies were computed at unfrozen-core aug-cc-pVTZ CCSD(T) optimized geometries: r(O–H) = 0.958 85 (0.934 11) Å and $\angle$(H–O–H) = 104.343 (180.0)° in the $C_{2v}(D_{\infty h})$ cases. See footnote a of Table I for an explanation of the layout of the focal-point analysis.

[b]The corresponding cc-pV*X*Z{RHF, δ[MP2], δ[CCSD], δ[CCSD(T)]}//cc-pV*X*Z CCSD(T) data are {12094, 505, 167, 106} and {11491, 134, 182, 58} cm^{-1}, respectively, in the X=D and T cases.

[c]Based on (X=4, 5, 6) cc-pV*X*Z RHF and MP2 total energies fit, respectively, to Eqs. (1) and (2) of the text.

the underlying basis set. For example, although the (X=3, 4, 5) cc-pV*X*Z δ[CCSD(T)] values of (+54, +17, −5) cm^{-1}, in order, show non-negligible variation, the corresponding (X=3, 4) aug-cc-pV*X*Z increments of (−11, −15) cm^{-1} are virtually constant. In correlation series (1, 2) the terms past (MP4, CCSD) amount to only (+23, −8) cm^{-1} in the aug-cc-pVTZ case, and the resulting ΔE_e(MP∞) and ΔE_e(CCSDT) values differ by a mere 5 cm^{-1}. Moreover, the focal-point extrapolation estimates from the perturbation and coupled-cluster series agree to within 17 cm^{-1}. Finally, due to error cancellation Hartree–Fock theory happens to give a very accurate barrier height, the disparity between the RHF and CCSDT ΔE_e values being as small as 9 cm^{-1} (cc-pV5Z case) and always less than 1%.

Sundry extrapolation schemes for ascertaining the complete-basis RHF and MP2 limits were also investigated for water. A fit of the exponential form of Eq. (1) to the (X=4, 5, 6) cc-pV*X*Z RHF total energies gives (−76.0673, −76.0161) E_h for the (C_{2v},$D_{\infty h}$) forms, consistent with previous Hartree–Fock estimates[14,89] for the bent structure. All-electron extrapolated energies already exist for water at different levels of electron correlation theory,[14] but our concern here is the valence focal-point analysis of relative energies. In the frozen-core MP2 case, the (X=4, 5, 6) cc-pV*X*Z correlation energies once again satisfy Eq. (2) much better than the (X=3, 4, 5) aug-cc-pV*X*Z set, providing the extrapolated δ[MP2] increment of −382 cm^{-1} assumed for the inversion barrier in Table II. As in the ammonia case, other treatments of the data suggest sizeable uncertainties ($\pm 0.5\, mE_h$) in the extrapolated second-order correlation energies. The alternate δ[MP2] values tend to be smaller in magnitude than in the preferred extrapolation, ranging downward to −320 cm^{-1}. The final focal-point results from series 1 and 2 for the inversion barrier become 11 129 and 11 112 cm^{-1}, respectively, with uncertainties of perhaps ± 60 cm^{-1}.

The relativistic correction for the inversion barrier of water (Table VI) is a positive number about twice as large as that of ammonia, in part because there are *two* stereochemically active lone electron pairs experiencing *sp* rehybridization.[96] The cc-pVTZ RHF, MP2, CCSD, and CCSD(T) predictions, as well as the cc-pVQZ CCSD result, all lie between +52 and +57 cm^{-1}. Likewise, the core correlation shift of the water barrier is substantially larger than for ammonia but not particularly sensitive to the level of theory. Considering the agreement among the MP2, CCSD, and CCSD(T) values for the cc-pCVTZ basis, the MP2 result of −106 cm^{-1} for the larger cc-pCVQZ set is adopted here. Therefore, the negative core correlation term, aided by the smaller (albeit significant) BODC shift of −17 cm^{-1}, again overcompensates for the positive relativistic correction. Partridge and Schwenke[89] have found that the sign and magnitude of the core correlation effect on the potential energy surface of water is strongly dependent on the geometry; their core correlation shift for the barrier is very similar to ours. In conclusion, the final prediction for the classical inversion barrier of water, assuming preference for the coupled-cluster valence focal-point series (Table II), is ΔE_e = 11 112 − 106 + 57 − 17 = 11 046 cm^{-1}, or 31.58 kcal mol^{-1}, perhaps with a ± 0.2 kcal mol^{-1} uncertainty. By comparison, the very recent, high-quality PJT2 spectroscopic potential[83,97] exhibits a 31.35 kcal mol^{-1} barrier, presenting only a very modest discrepancy for further resolution.

C. The inversion barrier of isocyanic acid

Widespread research has focused on the isocyanic acid molecule (HNCO) because of its role in the combustion chemistry of the $RAPRENO_x$ process, its emergence as a prototype for state-to-state reaction dynamics and mode-selective chemistry, its quasilinear spectroscopic behavior, and its presence in galactic radiation sources, *inter alia*.[62,98,99] The infrared spectrum of HNCO exhibits many challenging features and fascinating anomalies, most notably among the low-frequency vibrations, which experience large Coriolis coupling and centrifugal distortion engendered by

TABLE III. Valence focal-point analysis of the inversion barrier (ΔE_e, cm^{-1}) of isocyanic acid.[a]

		Series 1					Series 2			
	ΔE_e(RHF)	δ[MP2]	δ[MP3]	δ[MP4]	δ[MP5]	δ[MP∞]	ΔE_e(MP∞)	δ[CCSD]	δ[CCSD(T)]	δ[BD(TQ)]	ΔE_e[BD(TQ)]
cc-pVDZ (47)[b]	**1845**	+455	−125	+433	−254	+111	**2465**	+2	+188	−27	**2463**
cc-pCVDZ (59)	**1794**	+500	−137	+438	−264	+115	**2446**	−10	+187	−29	**2443**
cc-pVTZ/DZ (95)	**1569**	+201	−115	+395				+19	+151	[−27]	**[1913]**
cc-pVTZ (104)	**1569**	+267	−113	+382	[−254]	[+111]	**[1962]**	+5	+157	[−27]	**[1971]**
cc-pCVTZ (143)	**1567**	+303	−113					+2	+160		
aug-cc-pVTZ (161)	**1583**	+276	−106	+370				+14	+145		
cc-pVQZ (195)	**1568**	+201	−117	+378	[−254]	[+111]	**[1887]**	+4	+150	[−27]	**[1896]**
cc-pCVQZ (282)	**1567**	+217	−120								
aug-cc-pVQZ (286)	**1575**	+197	−121	+373				[+4]	[+150]		
cc-pV5Z (328)	**1564**	+189	−117	[+378]	[−254]	[+111]	**[1871]**	[+4]	[+150]	[−27]	**[1880]**
cc-pV6Z (511)	**1569**	+174	[−117]	[+378]	[−254]	[+111]	**[1861]**	[+4]	[+150]	[−27]	**[1870]**
Extrapolation limit (∞)[c]	**1570**	+167	[−117]	[+378]	[−254]	[+111]	**[1855]**	[+4]	[+150]	[−27]	**[1864]**

[a]All total energies were computed at unfrozen-core cc-pVTZ CCSD(T) optimized geometries: r(N–H) = 1.002 66 (0.984 73) Å, r(N═C) = 1.216 49 (1.179 37) Å, r(C═O) = 1.166 83 (1.176 80) Å, ∠(H–N═C) = 123.13 (180.0)°, and ∠(N═C═O) = 172.27 (180.0)° in the C_s($C_{\infty v}$) cases. See footnote a of Table I for an explanation of the layout of the focal-point analysis; however, correlation series 2 here is [RHF→MP2→CCSD→CCSD(T)→BD(TQ)].
[b]The corresponding cc-pVDZ {RHF, δ[MP2], δ[CCSD], δ[CCSD(T)]}//cc-pVDZ CCSD(T) data are {1870, 405, 43, 190} cm^{-1}.
[c]Based on (X = 4, 5, 6) cc-pVXZ RHF and MP2 total energies fit, respectively, to Eqs. (1) and (2) of the text.

the broad, flat H–N–C bending potential. These phenomena hinge on the barrier to linearity. Early spectroscopic work[100] suggested a value of 3600 ± 200 cm^{-1} for this inversion barrier. Several *ab initio* investigations[32,62,101] subsequently established a much lower barrier near that of ammonia, and a preliminary focal-point analysis,[32,62] including QZ($2d1f$,$2p1d$) CCSD(T) and PZ($3d2f$,$2p1d$) MP2 computations, predicted a height of 5.7 kcal mol^{-1} (2000 cm^{-1}). Then in 1995 a semirigid bender analysis[102] was performed on 543 ground-state rotational transitions, yielding an effective barrier of 1899 cm^{-1}. While the disparity between theory and experiment has thus diminished, no consensus exists on the precise barrier height.

Because the inversion of configuration at the nitrogen center is strongly coupled to electronic structural rearrangements in the π network of the NCO moiety, this problem provides a severe challenge for *ab initio* methods. The key manifestation of this π network coupling is focal-point behavior of the barrier (Table III) which is opposite that in the ammonia and water cases: modest one-particle basis set dependence but higher-order correlation series refractory toward convergence. The cc-pVDZ RHF barrier to linearity is 1845 cm^{-1}, whereas the successive MPn correlation increments from second through fifth order (+455, −125, +433, −254 cm^{-1}, in order) are strongly oscillatory, the net cc-pVDZ MP5 barrier being 2354 cm^{-1}. The lack of convergence in the successive cc-pVDZ MPn predictions is somewhat disconcerting and is substantiated by the +111 cm^{-1} value predicted via shifted Padé [2,1] approximants [Eq. (5)] for the remaining correlation error at fifth order. The estimated cc-pVDZ MP∞ value (2465 cm^{-1}) is supported by the remarkable agreement with the result (2463 cm^{-1}) derived from series 2, but it is necessary to extend the coupled-cluster treatment from CCSD(T) to the BD(TQ) level to achieve this accord. Despite the protracted correlation convergence of the barrier, both CASSCF and t_1 CCSD diagnostics reveal that HNCO does not exhibit a very high degree of multireference character.[62]

The contrasting approach to the complete basis set limit is evident first in the cc-pVXZ RHF sequence of inversion barriers. Application of Eq. (1) to the (X = 4, 5, 6) cc-pVXZ RHF data predicts −167.8450 (−167.8378) E_h as the Hartree–Fock limit for bent (linear) HNCO, thus providing an extrapolated barrier of 1570 cm^{-1} (Table III). Beginning with the small, mixed cc-pVTZ/DZ basis set, the computed RHF barriers do not deviate more than 13 cm^{-1} from the inferred limit, an unusual consistency rivaled in this study only by ethane. Past the cc-pVTZ/DZ point, the δ[MP2] contribution rises to +303 cm^{-1} before settling near +167 cm^{-1}, but its convergence is far more rapid than in the NH_3 and H_2O cases. The partitioning of the higher-order correlation increments is quite stable throughout the entire basis set sequence; e.g., the δ[MP3] term lies between −106 and −125 cm^{-1} in all cases except cc-pCVDZ. In the end, the valence focal-point extrapolation of series (1, 2) yields a barrier of (1855, 1864) cm^{-1}, with a preference perhaps for the series 2 result due to better correlation convergence.

As expected, the auxiliary corrections for HNCO are quite similar to their NH_3 counterparts, although the magnitudes of the adopted (cc-pVTZ CCSD) relativistic and (cc-pCVQZ MP2) core correlation shifts are about 30% larger. The BODC effect (ca. −10 cm^{-1}) is virtually identical for the two molecules. The final prediction for the classical inversion barrier of HNCO is thus $\Delta E_e = 1864 - 85 + 31 - 10 = 1800$ cm^{-1}, or 5.1 kcal mol^{-1}, which is about 0.6 kcal mol^{-1} smaller than the best previous theoretical result.[32,62] Comparison with the recent empirical barrier[102] of 1899 cm^{-1} is clouded by uncertainty over the zero-point averaging implicit in the semirigid bender (SRB) Hamiltonian, which generally does not treat vibrations complementary to the large-amplitude mode and specifically neglects the considerable Coriolis interactions among the lowest bending levels of HNCO. Harmonic vibrational frequencies are available from the DZ(d,p) RHF method for both linear and bent HNCO.[62] For the bent structure, these ω_i values predict an overall ZPVE(HNCO) which must be scaled by $\tau = 0.934$ to

TABLE IV. Valence focal-point analysis of the torsional barrier (ΔE_e, cm^{-1}) of ethane.[a]

		Series 1					Series 2			
	ΔE_e(RHF)	δ[MP2]	δ[MP3]	δ[MP4]	δ[MP5]	δ[MP∞]	ΔE_e(MP∞)	δ[CCSD]	δ[CCSD(T)]	δ[CCSDT]	ΔE_e(CCSDT)
cc-pVDZ (58)	**1153**	−13	−37	+5	−6	−1	**1101**	−43	−30	+33	**1101**
cc-pCVDZ (66)	**1151**	−11	−37	+6	−7	0	**1102**	−43	+5	−1	**1101**
cc-pVTZ/DZ (90)	**1085**	−46	−31	−1				−30	−5	−1	**1003**
cc-pVTZ (144)	**1061**	−45	−31	−3	[−6]	[−1]	**[975]**	−30	−7	−1	**978**
cc-pCVTZ (170)	**1059**	−48	−32	−3	[−6]	[−1]	**[969]**	−30	−7	[−1]	**[973]**
aug-cc-pVTZ (230)	**1063**	−52	−33	−5	[−6]	[−1]	**[966]**	−33	−8	[−1]	**[969]**
cc-pVQZ (290)	**1062**	−70	−31	−5	[−6]	[−1]	**[949]**	[−33]	[−8]	[−1]	**[950]**
cc-pCVQZ (348)	**1063**	−70									
aug-cc-pVQZ (436)	**1063**	−73	−30	[−5]	[−6]	[−1]	**[948]**	[−33]	[−8]	[−1]	**[948]**
cc-pV5Z (512)	**1063**	−68	[−30]	[−5]	[−6]	[−1]	**[953]**	[−33]	[−8]	[−1]	**[953]**
cc-pV6Z (826)	**1063**	[−68]	[−30]	[−5]	[−6]	[−1]	**[953]**	[−33]	[−8]	[−1]	**[953]**
Extrapolation limit (∞)[b]	**1063**	[−68]	[−30]	[−5]	[−6]	[−1]	**[953]**	[−33]	[−8]	[−1]	**[953]**

[a]The total energies were computed at unfrozen-core cc-pVTZ CCSD(T) optimized geometries: r(C═C) = 1.522 99 (1.537 26) Å, r(C–H) = 1.088 15 (1.087 08) Å and ∠(C–C–H) = 111.128 (111.576)° in the D_{3d}(D_{3h}) cases. See footnote a of Table I for an explanation of the layout of the focal-point analysis.

[b]Based on (X = 4, 5, 6) cc-pVXZ RHF total energies fit to Eq. (1) of the text, as well as assumed convergence of the cc-pV5Z δ[MP2] increment.

reproduce the accurate, anharmonic result ($4675\ cm^{-1}$)[62] surmised for this quantity. If the (ω_4, ω_5) bending mode is selected for assignment to the SRB large-amplitude coordinate, then the DZ(d,p) RHF frequency sets, scaled by τ, predict a ($+252, +120$) cm^{-1} zero-point effect on the barrier. In brief, the empirical barrier should translate into a vibrationless barrier in the 1600–1800 cm^{-1} range, whose upper but not lower portions would be in acceptable accord with our best focal-point extrapolation.

D. The torsional barrier of ethane

Paramount in vibrational studies of large-amplitude motion and in the calibration of molecular mechanics methods is the determination of conformational energy differences of small hydrocarbons and their chemical derivatives. The torsional barrier for restricted rotation about the C–C single bond in ethane constitutes a paradigm extensively studied over the last 60 years.[32,76,103–114] Early measurements of heat capacities pointed to an effective barrier of 962 cm^{-1}.[104] In the late 1960s, Weiss and Leroi[108] observed the torsional fundamentals and several hot bands of C_2H_6, CH_3CD_3, and C_2D_6, accounting for all of them with a one-term model potential exhibiting a barrier of 1024 cm^{-1}. In 1988, Moazzen-Ahmadi *et al.*[109] recorded and assigned 204($\Delta J = \pm 1$) infrared transitions between 225 and 340 cm^{-1} within the ν_4 fundamental and $2\nu_4 - \nu_4$ difference bands, subsequently applying a reduced vibration–torsion–rotation Hamiltonian to derive an empirical torsional potential with the Fourier coefficients (V_3, V_6) = (1011.890, 11.768) cm^{-1}. Two years earlier, Fantoni and co-workers[110] had identified a series of unresolved Q branches within the $2\nu_4$, $3\nu_4 - \nu_4$, $4\nu_4 - 2\nu_4$, and $5\nu_4 - 3\nu_4$ manifolds of the pure torsional Raman spectrum, thus probing vibrational states extending to the top of the torsional barrier and finding accord with a very similar Fourier potential. Accordingly, the best available effective torsional barrier (V_3) of ethane from experiment is 1012 cm^{-1}, which must be corrected for the zero-point vibrational energy of complementary modes before comparison with theory. For this purpose PZ($3d2f,2p1d$) MP2 harmonic frequencies of staggered and eclipsed ethane may be employed,[32] giving a $-59\ cm^{-1}$ vibrational shift and a bare empirical barrier of 953 cm^{-1}.

Theoretical considerations of internal rotation in ethane extend back to the ''precomputer'' work reviewed by Pitzer[104] and also include modern electronic structure analyses of the origin of the barrier.[106] Various *ab initio* computations[76,114] on ethane have also appeared, but relatively little work has incorporated substantial treatments of electron correlation. One high-quality prediction of the bare torsional barrier is 964 cm^{-1},[32] achieved by appending a QZ($2d1f,2p1d$)→PZ($3d2f,2p1d$) MP2 basis set shift to a QZ($2d1f,2p1d$) CCSD(T) result.

The current focal-point layout of the ethane barrier (Table IV) displays the most facile convergence toward the one- and n-particle limits seen in this study. Although the cc-pVDZ RHF barrier is 90 cm^{-1} too high, all basis sets past cc-pVTZ/DZ give RHF results within 4 cm^{-1} of the inferred Hartree–Fock limit given by the extrapolated total energies -79.2667(D_{3d}) and -79.2619(D_{3h}) E_h. The corresponding variation of the second-order correlation increment is considerably greater, approaching an apparent limit of $-68\ cm^{-1}$ rather slowly. In contrast, both the δ[MP3] and δ[CCSD] values of about $-30\ cm^{-1}$ are remarkably stable, consistent with the focal-point trends repeatedly observed here. The higher-order δ[MP4], δ[MP5], δ[CCSD(T)], and δ[CCSDT] terms are generally much less than 10 cm^{-1}, all becoming negative with larger basis sets. However, the anomalously large, albeit compensating, cc-pVDZ δ[CCSD(T)] and δ[CCSDT] values point out a danger in computing higher-order correlation increments with insufficiently flexible basis sets, even in well-behaved cases such as ethane. Finally, the equivalence of the net extrapolated barriers for series 1 and 2 (953 cm^{-1}) is remarkable.

Since rehybridization of valence electron pairs does not accompany torsional motion in ethane, both the relativistic ($+1.5\ cm^{-1}$) and core correlation ($+4\ cm^{-1}$) corrections to

the barrier are minuscule. In addition, the BODC effect ($-0.5\ \mathrm{cm}^{-1}$) is negligible. Applying these small shifts to the average valence focal-point barrier yields the final result $\Delta E_e = 953 + 1.5 + 4 - 0.5 = 958\ \mathrm{cm}^{-1}$ ($2.74\ \mathrm{kcal\ mol}^{-1}$), in excellent accord with the empirical value ($953\ \mathrm{cm}^{-1}$) inferred above. More extensive spectroscopic resolution, assignment, and fitting of torsional eigenstates, as well as an improved accounting of zero-point vibrational effects, is needed to reduce the small $5\ \mathrm{cm}^{-1}$ disparity. Nonetheless, the current accord for the ethane prototype, actualized by the nearly ideal focal-point convergence and the diminutive auxiliary shifts established here, presages the eventual computation of conformational barriers in small hydrocarbons to the $10\ \mathrm{cm}^{-1}$ level or better.

E. The *E*/*Z* rotamer separation of formic acid

As a fundamental building block of amino acids, the carboxylic functional group has been a prime target of conformational analysis. Recent theoretical studies[115–117] have shown that the factors heavily influencing the conformational energetics of simple neutral amino acids include not only various hydrogen bonding interactions but also the isomerization energy of the –COOH group. The prototype of this moiety is formic acid (HCOOH), one of the simplest molecules exhibiting rotational isomerism. Due to the delocalization of π electrons, both rotamers of HCOOH are planar, exhibiting Z/E arrangements of the carboxylic group, or *trans/cis* orientations of the hydrogen atoms. Extensive microwave spectroscopy[118–120] on formic acid isotopomers has established the geometric structures of both conformers. Infrared[121–124] and Raman[125] investigations have provided detailed vibrational assignments not only for formic acid monomers but also for its dimers, which are readily formed in the gas phase. The E/Z rotamer separation was the object of early disputes, but in 1976 microwave relative intensity measurements by Hocking[118] placed the E form $1365 \pm 30\ \mathrm{cm}^{-1}$ ($3.90 \pm 0.09\ \mathrm{kcal\ mol}^{-1}$) above its predominant, naturally occurring (Z) counterpart. This value remains uncontested and has been accepted in calibrations of molecular mechanics force fields.[126,127] Ostensibly the origin of the E/Z separation is intramolecular hydrogen bonding, but a similar energy difference in methylformate discounts this simple explanation, necessitating other plausible proposals.[128–130]

The numerous theoretical studies[128,131–135] prior to 1996 on geometric structures, vibrational force fields, and conformational energies of formic acid produced over thirty separate results for the E/Z isomerization energy, by means of sundry basis sets and established electronic structure methods including RHF, TCSCF, MP2-MP4, CEPA, and DFT. The Hartree–Fock predictions with basis sets up to 6-311 +G** in quality placed the E form as low as $1900\ \mathrm{cm}^{-1}$ above the Z minimum, but the rest of the uncorrelated values scattered higher over a range greater than $1000\ \mathrm{cm}^{-1}$. Correlation effects preferentially stabilize the E form; however, no MP*n* or DFT treatments reported prior to 1996 reduced the energy separation below $1600\ \mathrm{cm}^{-1}$.[128,134,135]

Accounting for zero-point vibrational effects fails to resolve the apparent discrepancy between theory and experiment. In particular, 4-31G and DZ RHF vibrational analyses[132] have given an $E-Z$ difference in ZPVE of $+90\ \mathrm{cm}^{-1}$, whereas more recent 6-31G** MP2 and DZVP2 NLSD harmonic frequencies[134] predict comparable magnitudes but opposite signs, viz., -98 and $-91\ \mathrm{cm}^{-1}$, respectively. This disparity led us to reevaluate the ZPVE effect by computing fully optimized cc-pVTZ MP2 harmonic frequencies $\{\omega_1-\omega_9\}$: {3761, 3123, 1819, 1421, 1318, 1138, 629, 1070, 688} cm^{-1} for Z-HCOOH and {3836, 3035, 1856, 1435, 1286, 1130, 661, 1046, 529} cm^{-1} for E-HCOOH. The higher-energy E form has larger O–H and C═O stretching frequencies but smaller C–H stretching and torsional frequencies, giving an $E-Z$ harmonic ZPVE difference of $-76\ \mathrm{cm}^{-1}$. For the Z rotamer the cc-pVTZ MP2 ω_i values overestimate the empirical fundamentals[121–123] by only 4% on average, bolstering confidence in the theoretical ZPVE shift and reducing concerns over anharmonic effects, whose proper reckoning is not feasible here. In summary, the empirical E/Z energy difference of Hocking[118] should correspond to a vibrationless separation near $1440 \pm 30\ \mathrm{cm}^{-1}$, well below the aforementioned spectrum of theoretical predictions.

The preliminary focal-point analysis by Császár[117] in 1996, which employed correlation-consistent basis sets and selected CCSD(T) computations, provided the first *ab initio* E/Z energy differences significantly below $1600\ \mathrm{cm}^{-1}$. This treatment is extended considerably toward completeness by the data in Table V. At the RHF level, the E/Z separation starts near $2000\ \mathrm{cm}^{-1}$ but falls precipitously with basis set augmentation. Even the cc-pVTZ→cc-pVQZ extension provides a substantial drop ($73\ \mathrm{cm}^{-1}$) in $\Delta E_e(E-Z)$, although subsequent reductions in the cc-pVXZ series amount to only $25\ \mathrm{cm}^{-1}$. The cc-pVXZ exponential extrapolations yield $-188.8603(Z)$ and $-188.8528(E)$ as estimates of the Hartree–Fock limit in E_h, corresponding to a rotamer separation of $1643\ \mathrm{cm}^{-1}$. Modest acceleration toward this limit is achieved by augmentation of the basis with diffuse shells, which in the $X=\{3, 4, 5\}$ cases results in (diminishing) ΔE_e(RHF) lowerings of $\{-84,-24,-8\}\ \mathrm{cm}^{-1}$, in order, and near equivalence of aug-cc-pVXZ and cc-pV$(X+1)$Z predictions. The δ[MP2] increment, which exhibits remarkably little variation, apparently converges to $-153\ \mathrm{cm}^{-1}$, virtually the same value given by the cc-pVTZ basis set. Its behavior is in stark contrast to that of the second-order correlation increment for the inversion barriers of NH_3 and H_2O, an observation suggesting that even though the oxygen lone pairs of formic acid have different repulsive interactions in the E and Z rotamers, there are no substantial differences in electronic structure.

The correlation increments past δ[MP2] for the E/Z separation of formic acid are generally larger than in the nearly ideal case of internal rotation in ethane, but not significantly so. The net [MP2→MP4,MP2→CCSD(T)] shifts are $(-43, -48)\ \mathrm{cm}^{-1}$ for the cc-pVDZ basis, but only $(-25, -9)\ \mathrm{cm}^{-1}$ for the aug-cc-pVTZ set. The extrapolation

TABLE V. Valence focal-point analysis of the E/Z rotamer separation (ΔE_e, cm^{-1}) of formic acid.[a]

			Series 1					Series 2			
	ΔE_e(RHF)	δ[MP2]	δ[MP3]	δ[MP4]	δ[MP5]	δ[MP∞]	ΔE_e(MP∞)	δ[CCSD]	δ[CCSD(T)]	δ[CCSDT]	ΔE_e(CCSDT)
cc-pVDZ (52)	**1995**	−120	−85	+42	−42	+14	**1804**	−48	0	−11	**1816**
cc-pCVDZ (64)	**1992**	−120	−83	+41	−42	+14	**1802**	−46	−1	−11	**1814**
cc-pVTZ/DZ (100)	**1784**	−106	−53	+25	[−42]	[+14]	**[1622]**	−26	−6	−8	**1638**
cc-pVTZ (118)	**1741**	−152	−43	+15	[−42]	[+14]	**[1533]**	−13	−10	[−8]	**[1558]**
cc-pCVTZ (157)	**1735**	−151						−13	−11	[−8]	**[1552]**
aug-cc-pVTZ (184)	**1657**	−171	−18	−7				+4	−13	[−8]	**[1469]**
cc-pVQZ (225)	**1668**	−150	−24	+5	[−42]	[+14]	**[1471]**	+1	−12	[−8]	**[1499]**
cc-pCVQZ (312)	**1668**	−151									
aug-cc-pVQZ (332)	**1644**	−157	−13	[+5]							
cc-pV5Z (383)	**1651**	−151	[−13]	[+5]	[−42]	[+14]	**[1464]**	[+1]	[−12]	[−8]	**[1481]**
aug-cc-pV5Z (541)	**1643**	−152	[−13]	[+5]				[+1]	[−12]	[−8]	**[1472]**
cc-pV6Z (602)	**1645**	−152	[−13]	[+5]	[−42]	[+14]	**[1457]**	[+1]	[−12]	[−8]	**[1474]**
Extrapolation limit (∞)[b]	**1643**	−153	[−13]	[+5]	[−42]	[+14]	**[1454]**	[+1]	[−12]	[−8]	**[1471]**

[a]All total energies were computed at unfrozen-core cc-pVTZ CCSD(T) optimized geometries: r(C–H) = 1.089 13 (1.095 46) Å, r(C═O) = 1.199 06 (1.192 69) Å, r(C–O) = 1.342 66 (1.348 98) Å, r(O–H) = 0.966 95 (0.961 63) Å, ∠(H–C═O) = 125.141 (123.892)°, ∠(O═C–O) = 125.057 (122.629)°, ∠(C–O–H) = 106.320 (108.580)°, and ∠(O═C–O–H) = 0 (180)° in the $Z(E)$ cases. See footnote a of Table I for an explanation of the layout of the focal-point analysis.

[b]Based on (X = 4, 5, 6) cc-pVXZ RHF and MP2 energies fit, respectively, to Eqs. (1) and (2) of the text.

from MP4 to MP∞ is only possible in the cc-pVDZ and cc-pCVDZ cases, in which this higher-order effect is predicted to be $-28\ cm^{-1}$. Considering the observed diminution of the third- and fourth-order correlation shifts with basis set augmentation, this $-28\ cm^{-1}$ estimate is probably too large; *n.b.*, the corresponding CCSD(T)→CCSDT change is only $-11\ cm^{-1}$. Accordingly, the difference between the series 1 and 2 extrapolations is larger on a percentage basis for formic acid than in the other systems analyzed above. Assuming preference for the coupled-cluster approach, a final valence focal-point result of $1471\ cm^{-1}$ is obtained for the E/Z rotamer separation.

Because the electronic structures of the Z and E torsional isomers of formic acid are so similar, both the relativistic and core correlation corrections are $1\ cm^{-1}$ or less in magnitude (Table VI). Including these minuscule effects, as well as the small BODC shift ($+4\ cm^{-1}$), the final E/Z energy difference is predicted to be $1474\ cm^{-1}$, at the upper edge of the uncertainty interval of the empirically based vibrationless result ($1440 \pm 30\ cm^{-1}$). As such, the current analysis constitutes the first *ab initio* validation of a rotamer separation as small as that deduced by Hocking in 1976.[118]

F. Other systems

Diversity is added to the current survey of conformational energy prototypes by highlighting some of our recent work on the torsional conformations of butane[35] and the polytopic potential energy surface of silicon dicarbide (SiC_2).[136] For the *anti/syn* carbon backbone torsional barrier of butane, a valence focal-point analysis was executed by means of DZP MP2→[13*s*8*p*6*d*4*f*/8*s*6*p*4*d*] MP2 and TZ(2*d*,2*p*) RHF→TZ(2*d*,2*p*) CCSD(T) computations at DZP CISD optimum structures. The basis-set series was less systematic than the correlation-consistent sets used here, because spherical harmonics past *f* functions could not be employed in direct MP2 procedures at the time, but it was possible to advance an *anti/syn* barrier of 5.40 $\pm 0.15\ kcal\ mol^{-1}$. The focal-point characteristics of the *anti/syn* energy difference in butane are similar to those ob-

TABLE VI. Non-Born–Oppenheimer (BODC), relativistic, and core correlation shifts (cm^{-1}) on conformational energy prototypes.[a]

	BODC	Relativistic effects			Core correlation			
	DZP RHF	cc-pVTZ RHF	cc-pVTZ MP2	cc-pVTZ CCSD	cc-pCVTZ MP2	cc-pCVQZ MP2	cc-pCVTZ CCSD	cc-pCVTZ CCSD(T)
NH_3	−10.7	+22.5	+22.6	+22.6	−56	−64	−54	−53
H_2O[b]	−16.6	+52.8	+56.5	+56.8	−96	−106	−89	−87
HNCO	−9.7	+34.0	+30.1	+30.5	−74	−85	−78	−78
C_2H_6	−0.5	+1.1	+1.5		+3	+4	+4	+4
HCOOH	+3.9	+0.1	+0.3		+1	+1	+1	−1
SiC_2	−6.3	−14.9	−34.7	−28.8	+112[c]			

[a]The energetic quantities of concern are the inversion barriers of NH_3, H_2O, and HNCO, the torsional barrier of C_2H_6, the E/Z rotamer separation of HCOOH, and the barrier to linearity of SiC_2.

[b]Additional relativistic shifts for water: cc-pVQZ CCSD = +54.8 and cc-pVTZ CCSD(T) = +57.1 cm^{-1}.

[c]In this case the silicon basis was constructed from its cc-pVTZ antecedent by completely uncontracting the *sp* space and adding two tight *d* and *f* sets via successive extension of the polarization manifolds into the core region with a geometric ratio of 3.0.

served here for ethane: rapid Hartree–Fock convergence, protracted variations in δ[MP2], and very stable higher-order increments. The definitive *ab initio* results for butane provided a benchmark for testing the limits of transferability of potential functions utilized in molecular mechanics schemes such as MM4, as well as a critique of spectroscopically derived torsional potentials exhibiting questionable *anti/syn* barriers.

In the SiC_2 study,[136] long-standing problems of the topography, energetics, and vibrational dynamics of the ground-state surface were systematically addressed. The silicon dicarbide system exhibits a mercurial surface for the circumnavigation of Si^+ about C_2^- in that almost all conceivable variations with level of theory are observed. In the end, the global minimum of SiC_2 is a T-shaped (C_{2v}) structure connected monotonically to a linear Si–C–C transition state, the bent transition states and L-shaped minima appearing at quite high levels of theory ultimately becoming spurious. Instructive here is the barrier to linearity for T-shaped SiC_2 [Δ(L–T)], a pathological case of focal-point convergence. With a modest DZ(d) basis, Δ(L–T) is predicted at the (RHF, MP2) level to be $(-5.09, +2.63)$ kcal mol^{-1}, whereas the ensuing Δ(L–T) values in the (MP3, MP4, MP5, MP∞) and [CCSD, CCSD(T), BD(TQ)] correlation series are $(+1.73, -1.63, +1.87, +0.58)$ and $(+1.64, +0.15, +1.26)$ kcal mol^{-1}, in order. Moreover, the ($X=3, 4, 5$) cc-pVXZ MP2 results are $\Delta(\text{L–T}) = (+5.48, +6.21, +6.59)$ kcal mol^{-1}. In brief, the SiC_2 problem presents both disturbingly oscillatory higher-order correlation series *and* protracted convergence of the δ[MP2] increment.

To augment the SiC_2 analysis, a few additional computations were undertaken here. First, Δ(L–T) values of $+0.64$ and $+0.54$ kcal mol^{-1} were obtained at the cc-pVDZ CCSD(T) and CCSDT levels, respectively, showing that a complete rather than perturbative treatment of the connected triple excitations hardly changes the energetic predictions. Second, the earlier extrapolation[136] of ($X=3, 4, 5$) cc-pVXZ MP2 energies on the basis of a geometric progression was replaced with a fit of these data to Eq. (2). The complete-basis valence second-order correlation energy estimates thereby increase in size by 1–2 mE_h to $(-0.4081, -0.4170)$ E_h for (linear, T-shaped) SiC_2, but the δ[MP2] increment to Δ(L–T) actually decreases, giving a limiting MP2 barrier to linearity of 6.74 rather than 7.02 kcal mol^{-1}. Finally, the relativistic, core-correlation, and BODC shifts were evaluated as -0.08, $+0.32$, and -0.02 kcal mol^{-1} (Table VI) at the cc-pVTZ CCSD, cc-pCVTZ MP2, and DZP RHF levels of theory, respectively. The 0.28 kcal mol^{-1} reduction in the estimate of the limiting MP2 barrier is thus compensated by a 0.22 kcal mol^{-1} increase due to the auxiliary shifts, and the earlier proposal of 5.8 kcal mol^{-1} is not significantly altered. However, if the CCSD(T)/CCSDT accord is considered to vitiate the substantial correction suggested by the CCSD(T)$\rightarrow$MP∞ extrapolation in this system,[136] then the predicted barrier to linearity of SiC_2 would be reduced to 5.3 kcal mol^{-1}. In this event, agreement would be improved with the empirical barrier (5.4 kcal mol^{-1}) of Ross and co-workers,[137] who in 1994 fitted a semirigid bender potential to vibrational overtones up to $(v_1, v_2, v_3) = (0,0,14)$ observed by stimulated emission pumping (SEP) of the $\tilde{X}\ ^1A_1/\tilde{A}\ ^1B_2$ system.

TABLE VII. Summary of diverse convergence behavior of conformational energy prototypes.[a]

	Basis set variation past cc-pVQZ[b]	Largest correlation increment past MP4[c]
NH_3	>200	$\leqslant 30$
H_2O	>350	<25
HNCO	<30	>250
C_2H_6	<5	<10
HCOOH	<30	<45
SiC_2	>280	>380

[a]All entries in cm^{-1}. The energetic quantities of concern are the inversion barriers of NH_3, H_2O, and HNCO, the torsional barrier of C_2H_6, the E/Z rotamer separation of HCOOH, and the barrier to linearity of SiC_2.
[b]Measured as the difference between ΔE_e(MP∞) for the cc-pVQZ set and the corresponding estimate in the complete basis set limit.
[c]Gauged by the δ[MP5] and δ[MP∞] values obtained with the largest feasible basis set.

IV. CONCLUSIONS

(1) The molecules considered in this work exhibit the gamut of focal-point behavior for relative energies, providing plentiful instruction in the pursuit of the *ab initio* limit. As summarized in Table VII, the diverse (basis set, correlation) convergence may be characterized as follows: NH_3 and H_2O inversion barriers (poor, good); HNCO inversion barrier (good, poor); C_2H_6 and HCOOH torsional energetics (good, good); and SiC_2 barrier to linearity (poor, poor). The behavior of the various correlation series is noteworthy because in none of these systems may the electronic structure be considered multireference in nature by traditional standards; moreover, in all cases the iterative full CCSDT and perturbative CCSD(T) predictions are virtually identical.

(2) Considerable variations in the RHF and MP2 predictions for the conformational energy prototypes are observed upon systematic enlargement of the one-particle basis set, but usually only small changes are seen in the higher-order correlation contributions to these quantities. The final extrapolations show that in the basis set limit, the (RHF, MP2) level yields (90, 92)%, (101, 98)%, (84, 93)%, (111, 104)%, and (112, 102)% of the relative energies (ΔE_e) in the NH_3, H_2O, HNCO, C_2H_6, and HCOOH cases, in order. For these molecules the representative cc-pVTZ$\rightarrow$cc-pVQZ augmentation engenders average changes in the RHF, δ[MP2], and higher-order contributions to ΔE_e of 2.6%, 2.6%, and 0.3%, respectively, in accord with the focal-point concept.[31–35] The results reveal that for some inversion barriers the δ[MP2] increment may not converge within even a modest 0.1 kcal mol^{-1} target until the basis set is extended drastically, i.e., to the cc-pV6Z level or beyond.

(3) The augmentation scheme for the correlation-consistent basis sets greatly improves the description of the inversion barriers in ammonia and water, which are dominated by rehybridization effects and variations in the dif-

fuseness of lone electron pairs. For example, the aug-cc-pVTZ RHF barrier for (NH_3, H_2O) lies within (19, 34) cm^{-1} of the Hartree–Fock limit, whereas the corresponding cc-pVTZ result is (124, 273) cm^{-1} too high. In both the MP*n* and coupled-cluster correlation series, the aug-cc-pVXZ basis sets prove commensurate in accuracy with the larger cc-pV($X+1$)Z sets. Although concern has recently arisen regarding possible divergence of *augmented* cc-pV*X*Z *absolute* MP*n* correlation energy series,[138] smooth convergence patterns are observed in the focal-point analyses of the inversion barriers.

(4) Extrapolation schemes for deducing Hartree–Fock and correlation energies in the one-particle basis set limit are meritorius for improved conformational energy predictions, but genuine spectroscopic accuracy to the 1 cm^{-1} level currently appears out of reach for most problems, even with directly computed total energies through the cc-pV6Z milestone. In particular, variations in the total energies extrapolated by several well-based procedures place uncertainties in the 0.05–0.10 kcal mol^{-1} range for the inversion barriers investigated here. The ($X=4$, 5, 6) cc-pV*X*Z MP2 energies fit Eq. (2) an order of magnitude better than the ($X=3$, 4, 5) aug-cc-pV*X*Z MP2 sets in the NH_3 and H_2O cases, notwithstanding the importance of diffuse functions in obtaining accurate barrier heights. This observation suggests that asymptotic forms such as Eq. (2) are not likely to be strongly operative until the cc-pVQZ level or beyond.

(5) While the full recovery of the core correlation energy is a daunting task, its effect on the relative energies of molecular conformations may be accurately predicted in many cases with cc-pCV*X*Z basis sets even at the MP2 level of theory. For example, correlation of the core electrons via the cc-pCVTZ MP2, CCSD, and CCSD(T) methods reduces the inversion barrier of ammonia by 56, 54, and 53 cm^{-1}, respectively. Such observations adduce the use of direct-MP2 methods to effectively determine core correlation shifts in larger systems.

(6) The size of the relativistic effect for conformational changes appears to be integrally related to the extent of attendant *sp* rehybridization for stereochemically active lone electron pairs. The torsional motions for internal rotation in ethane and formic acid entail no rehybridization, and thus the relativistic shift is less than 5 cm^{-1}. The inversion barriers in NH_3 and HNCO involve substantial changes in the *sp* character of one nitrogen lone electron pair, engendering a 20–30 cm^{-1} stabilization of the *s*-rich pyramidal form. An analogous rehybridization occurs for inversion in H_2O, but two lone pairs are involved, and indeed the relativistic stabilization of the bent structure is roughly twice as large.

(7) Non-Born–Oppenheimer shifts on barriers and conformational energies may be either positive or negative. The magnitude of the first-order BODC effect is between 9 and 17 cm^{-1} for the inversion problems studied here and less than 4 cm^{-1} for the C_2H_6 and HCOOH torsional cases.

(8) The extensive valence focal-point analyses presented here, amended by corrections for core correlation, special relativity, and the Born–Oppenheimer approximation, yield the following final predictions for relative energies: the classical inversion barriers of NH_3, H_2O, and HNCO are 5.026, 31.58, and 5.1 kcal mol^{-1}, in order; the bare torsional barrier of ethane is 2.74 kcal mol^{-1}; and the vibrationless *E*/*Z* isomerization energy of formic acid is 4.21 kcal mol^{-1}. Accounting for zero-point vibrational effects by *ab initio* methods brings the barriers for ammonia and ethane to within 0.05 kcal mol^{-1} of effective one-dimensional barriers from experiment.

ACKNOWLEDGMENTS

This paper is dedicated to Professor Normal L. Allinger. The work of A. G. Császár is partially supported by the Hungarian Ministry of Culture and Education (MKM/517 and FKFP 0117/1997) and by the Scientific Research Foundation of Hungary (OTKA T024044). The authors thank Dr. Yukio Yamaguchi for assistance with the BODC computations.

[1] E. L. Eliel, N. L. Allinger, S. J. Angyal, and G. A. Morrison, *Conformational Analysis* (American Chemical Society, Washington D.C., 1965).
[2] K. Raghavachari and L. A. Curtiss, in *Modern Electronic Structure Theory, Part II*, edited by D. R. Yarkony (World Scientific, Singapore, 1995); L. A. Curtiss, K. Raghavachari, G. W. Trucks, and J. A. Pople, J. Chem. Phys. **94**, 7221 (1991).
[3] G. A. Petersson and M. Braunstein, J. Chem. Phys. **83**, 5129 (1985); G. A. Petersson, A. Bennett, T. G. Tensfeldt, M. A. Al-Laham, W. A. Shirley, and J. Mantzaris, *ibid.* **89**, 2193 (1988); J. W. Ochterski, G. A. Petersson, and J. A. Montgomery, Jr., J. Am. Chem. Soc. **117**, 11299 (1995).
[4] J. M. L. Martin, J. Chem. Phys. **97**, 5012 (1992); **100**, 8186 (1994).
[5] P. E. M. Siegbahn, M. R. A. Blomberg, and M. Svensson, Chem. Phys. Lett. **223**, 35 (1994); P. E. M. Siegbahn, M. Svensson, and P. J. E. Boussard, J. Chem. Phys. **102**, 5377 (1995).
[6] C. Schwartz, Phys. Rev. **126**, 1015 (1962).
[7] D. P. Carroll, H. J. Silverstone, and R. M. Metzger, J. Chem. Phys. **71**, 4142 (1979).
[8] W. Kutzelnigg and J. D. Morgan III, J. Chem. Phys. **96**, 4484 (1992); **97**, 8821E (1992).
[9] T. H. Dunning, Jr., J. Chem. Phys. **90**, 1007 (1989).
[10] R. A. Kendall, T. H. Dunning, Jr., and R. J. Harrison, J. Chem. Phys. **96**, 6796 (1992).
[11] D. E. Woon and T. H. Dunning, Jr., J. Chem. Phys. **98**, 1358 (1993); **100**, 2975 (1994); **103**, 4572 (1995); A. K. Wilson, T. v. Mourik, and T. H. Dunning, Jr., J. Mol. Struct. THEOCHEM **388**, 339 (1997).
[12] See also A. D. Pradhan, H. Partridge, C. W. Bauschlicher, Jr., J. Chem. Phys. **101**, 3857 (1994).
[13] D. Feller, J. Chem. Phys. **96**, 6104 (1992); **98**, 7059 (1993).
[14] T. Helgaker, W. Klopper, H. Koch, and J. Noga, J. Chem. Phys. **106**, 9639 (1997).
[15] J. M. L. Martin, Chem. Phys. Lett. **259**, 669 (1996).
[16] J. A. Pople, M. J. Frisch, B. T. Luke, and J. S. Binkley, Int. J. Quantum Chem., Symp. **17**, 307 (1983).
[17] F. Brändas and O. Goscinski, Phys. Rev. A **1**, 552 (1970); O. Goscinski, Int. J. Quantum Chem. **1**, 769 (1967); S. Wilson, *ibid.* **18**, 905 (1980).
[18] W. D. Laidig, G. Fitzgerald, and R. J. Bartlett, Chem. Phys. Lett. **113**, 151 (1985); R. J. Bartlett and I. Shavitt, *ibid.* **50**, 190 (1977).
[19] N. C. Handy, P. J. Knowles, and K. Somasundram, Theor. Chim. Acta **68**, 87 (1985); C. Schmidt, M. Warken, and N. C. Handy, Chem. Phys. Lett. **211**, 272 (1993).
[20] D. Cremer and Z. He, J. Phys. Chem. **100**, 6173 (1996); Z. He and D. Cremer, Int. J. Quantum Chem. **59**, 71 (1996).
[21] P. Claverie, S. Diner, and J. P. Malrieu, Int. J. Quantum Chem. **1**, 751 (1967); B. Huron, J. P. Malrieu, and P. Rancurel, J. Chem. Phys. **58**, 5745 (1973); S. Evangelisti, J. P. Daudey, and J. P. Malrieu, Chem. Phys. **75**, 91 (1983).
[22] Z. Gershgorn and I. Shavitt, Int. J. Quantum Chem. **2**, 751 (1968).
[23] C. F. Bender and E. R. Davidson, Phys. Rev. **183**, 23 (1969).

[24] R. J. Buenker and S. D. Peyerimhoff, Theor. Chim. Acta **35**, 33 (1974); **39**, 217 (1975); R. J. Buenker, S. D. Peyerimhoff, and W. Butscher, Mol. Phys. **35**, 771 (1978); P. J. Bruna, S. D. Peyerimhoff, and R. J. Buenker, Chem. Phys. Lett. **72**, 278 (1980).
[25] R. J. Harrison, J. Chem. Phys. **94**, 5021 (1991).
[26] A. V. Luzanov, A. L. Wulfov, and V. O. Krouglov, Chem. Phys. Lett. **197**, 614 (1992).
[27] A. L. Wulfov, Chem. Phys. Lett. **255**, 300 (1996); **263**, 79 (1996).
[28] W. Klopper and W. Kutzelnigg, Chem. Phys. Lett. **134**, 17 (1987); J. Noga and W. Kutzelnigg, J. Chem. Phys. **101**, 7738 (1994); W. Klopper and J. Noga, *ibid.* **103**, 6127 (1995); R. J. Gdanitz, Chem. Phys. Lett. **210**, 253 (1993).
[29] S. F. Boys, Proc. R. Soc. London, Ser. A **258**, 402 (1960); K. Singer, *ibid.* **258**, 412 (1960).
[30] W. Cencek and J. Rychlewski, J. Chem. Phys. **98**, 1252 (1993); R. Bukowski, B. Jeziorski, S. Rybak, and K. Szalewicz, *ibid.* **102**, 888 (1995); B. J. Persson and P. R. Taylor, *ibid.* **105**, 5915 (1996).
[31] A. L. L. East and W. D. Allen, J. Chem. Phys. **99**, 4638 (1993).
[32] W. D. Allen, A. L. L. East, and A. G. Császár, in *Structures and Conformations of Non-Rigid Molecules*, edited by J. Laane, M. Dakkouri, B. van der Veken, and H. Oberhammer (Kluwer, Dordrecht, 1993).
[33] B. D. Wladkowski, W. D. Allen, and J. I. Brauman, J. Phys. Chem. **98**, 13532 (1994).
[34] S. J. Klippenstein, A. L. L. East, and W. D. Allen, J. Chem. Phys. **105**, 118 (1996).
[35] N. L. Allinger, J. T. Fermann, W. D. Allen, and H. F. Schaefer, J. Chem. Phys. **106**, 5143 (1997).
[36] J. M. L. Martin, Chem. Phys. Lett. **242**, 343 (1995).
[37] A. G. Császár and W. D. Allen, J. Chem. Phys. **104**, 2746 (1996); A. G. Császár, J. Phys. Chem. **98**, 8823 (1994).
[38] C. W. Bauschlicher, Jr. and H. Partridge, J. Chem. Phys. **100**, 4329 (1994); C. W. Bauschlicher, Jr. and S. R. Langhoff, *ibid.* **88**, 2540 (1988).
[39] A. L. L. East and L. Radom, J. Mol. Struct. **376**, 437 (1996).
[40] K. Balasubramanian, *Relativistic Effects in Chemistry, Part A: Theory and Techniques* and *Part B: Applications* (Wiley, New York, 1997).
[41] A. Fröman, Phys. Rev. **112**, 870 (1958); J. P. Desclaux, Comput. Phys. Commun. **9**, 31 (1975); P. Pyykkö, Adv. Quantum Chem. **11**, 353 (1978); Chem. Rev. **88**, 563 (1988); I. P. Grant and H. M. Quiney, Adv. At. Mol. Phys. **23**, 37 (1988); R. D. Cowan and D. C. Griffin, J. Opt. Soc. Am. **66**, 1010 (1976).
[42] P. Schwerdtfeger, L. J. Laakkonen, and P. Pyykkö, J. Chem. Phys. **96**, 6807 (1992).
[43] K. G. Dyall, P. R. Taylor, K. Faegri, Jr., and H. Partridge, J. Chem. Phys. **95**, 2583 (1991).
[44] S. A. Perera and R. J. Bartlett, Chem. Phys. Lett. **216**, 606 (1993).
[45] N. C. Handy, Y. Yamaguchi, and H. F. Schaefer, J. Chem. Phys. **84**, 4481 (1986).
[46] H. Sellers and P. Pulay, Chem. Phys. Lett. **103**, 463 (1984); W. Cencek and W. Kutzelnigg, Chem. Phys. Lett. **266**, 383 (1997).
[47] C. C. J. Roothaan, Rev. Mod. Phys. **23**, 69 (1951).
[48] W. J. Hehre, L. Radom, P. v. R. Schleyer, and J. A. Pople, *Ab Initio Molecular Orbital Theory* (Wiley-Interscience, New York, 1986); A. Szabo and N. S. Ostlund, *Modern Quantum Chemistry: Introduction to Advanced Electronic Structure Theory*, 1st ed., revised (McGraw-Hill, New York, 1989).
[49] J. A. Pople, J. S. Binkley, and R. Seeger, Int. J. Quantum Chem., Symp. **10**, 1 (1976); R. Krishnan and J. A. Pople, Int. J. Quantum Chem. **14**, 91 (1978); R. Krishnan, M. J. Frisch, and J. A. Pople, J. Chem. Phys. **72**, 4244 (1980).
[50] K. Raghavachari, J. A. Pople, E. S. Replogle, and M. Head-Gordon, J. Phys. Chem. **94**, 5579 (1990).
[51] R. J. Bartlett, Annu. Rev. Phys. Chem. **32**, 359 (1981); R. J. Bartlett, C. E. Dykstra, and J. Paldus, in *Advanced Theories and Computational Approaches to the Electronic Structure of Molecules*, edited by C. E. Dykstra (Reidel, Dordrecht, 1983), p. 127.
[52] G. E. Scuseria, A. C. Scheiner, T. J. Lee, J. E. Rice, and H. F. Schaefer, J. Chem. Phys. **86**, 2881 (1987); A. C. Scheiner, G. E. Scuseria, J. E. Rice, T. J. Lee, and H. F. Schaefer, *ibid.* **87**, 5361 (1987).
[53] J. Noga and R. J. Bartlett, J. Chem. Phys. **86**, 7041 (1987); **89**, 3401E (1988); G. E. Scuseria and H. F. Schaefer, Chem. Phys. Lett. **152**, 382 (1988).
[54] K. Raghavachari, G. W. Trucks, J. A. Pople, and M. Head-Gordon, Chem. Phys. Lett. **157**, 479 (1989); G. E. Scuseria and T. J. Lee, J. Chem. Phys. **93**, 5851 (1990).
[55] N. C. Handy, J. A. Pople, M. Head-Gordon, K. Raghavachari, and G. W. Trucks, Chem. Phys. Lett. **164**, 185 (1989).
[56] C. L. Janssen, E. T. Seidl, G. E. Scuseria, T. P. Hamilton, Y. Yamaguchi, R. B. Remington, Y. Xie, G. Vacek, C. D. Sherrill, T. D. Crawford, J. T. Fermann, W. D. Allen, B. R. Brooks, G. B. Fitzgerald, D. J. Fox, J. F. Gaw, N. C. Handy, W. D. Laidig, T. J. Lee, R. M. Pitzer, J. E. Rice, P. Saxe, A. C. Scheiner, and H. F. Schaefer III, PSI 2.0.8 (PSITECH Inc., Watkinsville, GA, 1994).
[57] M. J. Frisch, G. W. Trucks, H. B. Schlegel, P. M. W. Gill, B. G. Johnson, M. A. Robb, J. R. Cheeseman, T. Keith, G. A. Petersson, J. A. Montgomery, K. Raghavachari, M. A. Al-Laham, V. G. Zakrzewski, J. V. Ortiz, J. B. Foresman, J. Cioslowski, B. B. Stefanov, A. Nanayakkara, M. Challacombe, C. Y. Peng, P. Y. Ayala, W. Chen, M. W. Wong, J. L. Andres, E. S. Replogle, R. Gomperts, R. L. Martin, D. J. Fox, J. S. Binkley, D. J. Defrees, J. Baker, J. P. Stewart, M. Head-Gordon, C. Gonzalez, and J. A. Pople, GAUSSIAN 94, Revision C.3 (Gaussian, Inc., Pittsburgh, PA, 1995).
[58] J. F. Stanton, J. Gauss, W. J. Lauderdale, J. D. Watts, and R. J. Bartlett, ACES II. The package also contains modified versions of the MOLECULE Gaussian integral program of J. Almlöf and P. R. Taylor, the ABACUS integral derivative program written by T. U. Helgaker, H. J. Aa. Jensen, P. Jørgensen, and P. R. Taylor, and the PROPS property evaluation integral code of P. R. Taylor.
[59] T. J. Lee and A. P. Rendell, J. Chem. Phys. **94**, 6229 (1991); G. E. Scuseria, *ibid.* **94**, 442 (1991); J. D. Watts, J. Gauss, and R. J. Bartlett, Chem. Phys. Lett. **200**, 1 (1992).
[60] J. L. Duncan and I. M. Mills, Spectrochim. Acta **20**, 523 (1964).
[61] *Structure Data of Free Polyatomic Molecules*, edited by K. Kuchitsu (Springer, Berlin, 1995), Vol. 23.
[62] A. L. L. East, C. S. Johnson, and W. D. Allen, J. Chem. Phys. **98**, 1299 (1993).
[63] J. D. Swalen and J. A. Ibers, J. Chem. Phys. **36**, 1914 (1962).
[64] W. T. Weeks, K. T. Hecht, and D. M. Dennison, J. Mol. Spectrosc. **8**, 30 (1962).
[65] J. E. Wollrab, *Rotational Spectra and Molecular Structure* (Academic, New York, 1967).
[66] B. Maessen, P. Bopp, D. R. McLaughlin, and M. Wolfsberg, Z. Naturforsch. Teil A **39**, 1005 (1984).
[67] P. Bopp, D. R. McLaughlin, and M. Wolfsberg, Z. Naturforsch. Teil A **37**, 398 (1982).
[68] D. Papoušek and V. Špirko, Top. Curr. Chem. **68**, 59 (1976), and references therein; V. Špirko, J. Mol. Spectrosc. **101**, 30 (1983); V. Špirko and W. P. Kraemer, *ibid.* **133**, 331 (1989).
[69] A. Rauk, L. C. Annel, and E. Clementi, J. Chem. Phys. **52**, 4133 (1970).
[70] R. M. Stevens, J. Chem. Phys. **61**, 2086 (1974).
[71] M. F. Guest and S. Wilson, Chem. Phys. Lett. **72**, 49 (1980).
[72] W. R. Rodwell and L. Radom, J. Chem. Phys. **72**, 2205 (1980).
[73] P. R. Bunker, W. P. Kraemer, and V. Spirko, Can. J. Phys. **62**, 1801 (1984).
[74] T. J. Lee, R. B. Remington, Y. Yamaguchi, and H. F. Schaefer, J. Chem. Phys. **89**, 408 (1988).
[75] G. Campoy, A. Palma, and L. Sandoval, Int. J. Quantum Chem., Quantum Chem. Symp. **23**, 355 (1989); P. E. S. Wormer, E. H. T. Olthof, R. A. H. Engelm, and J. Reuss, Chem. Phys. **178**, 189 (1993); K. S. Werpetinski and M. Cook, Phys. Rev. A **52**, 3397 (1995).
[76] F. Jensen, Chem. Phys. Lett **261**, 633 (1996); J. S. Lee, J. Phys. Chem. A **101**, 8762 (1997).
[77] D. J. Rush and K. B. Wiberg, J. Phys. Chem. A **101**, 3143 (1997).
[78] J. M. L. Martin, T. J. Lee, and P. R. Taylor, J. Chem. Phys. **97**, 8361 (1992).
[79] L. Wallace, P. F. Bernath, W. Livingston, K. Hinkle, J. Busler, B. Guo, and K. Zhang, Science **268**, 1155 (1995).
[80] W. S. Benedict, N. Gailar, and E. K. Plyler, J. Chem. Phys. **24**, 1139 (1956).
[81] A. G. Császár and I. M. Mills, Spectrochim. Acta A **53**, 1101 (1997).
[82] A. B. McCoy and E. L. Sibert III, J. Chem. Phys. **92**, 1893 (1990).
[83] O. L. Polyansky, P. Jensen, and J. Tennyson, J. Chem. Phys. **101**, 7651 (1994); **105**, 6490 (1996).
[84] S. Carter and N. C. Handy, Mol. Phys. **47**, 1445 (1982); J. Chem. Phys. **87**, 4294 (1987).
[85] L. Halonen and T. Carrington, Jr., J. Chem. Phys. **88**, 4171 (1988).
[86] O. L. Polyansky, N. F. Zobov, S. Viti, J. Tennyson, P. F. Bernath, and L. Wallace, Science **277**, 346 (1997).
[87] O. L. Polyansky, N. F. Zobov, J. Tennyson, J. A. Lotoski, and P. F. Bernath, J. Mol. Spectrosc. **184**, 35 (1997).

[88] O. N. Ulenikov and G. A. Ushakova, J. Mol. Spectrosc. **117**, 195 (1986).
[89] H. Partridge and D. W. Schwenke, J. Chem. Phys. **106**, 4618 (1997).
[90] D. Moncrieff and S. Wilson, J. Phys. B **29**, 6009 (1996); J. S. Lee, J. Chem. Phys. **106**, 4022 (1997).
[91] R. J. Bartlett, S. J. Cole, G. D. Purvis, W. C. Ermler, H. C. Hsieh, and I. Shavitt, J. Chem. Phys. **87**, 6579 (1987).
[92] W. H. Green, A. Willetts, D. Jayatilaka, and N. C. Handy, Chem. Phys. Lett. **169**, 127 (1990); W. Gabriel, E. A. Reinsch, P. Rosmus, S. Carter, and N. C. Handy, J. Chem. Phys. **99**, 897 (1993).
[93] J. M. L. Martin, J. P. Francois, and R. Gijbels, J. Chem. Phys. **95**, 8374 (1991).
[94] H. G. Kjaergaard, B. R. Henry, H. Wei, S. Lefebvre, T. Carrington, O. S. Mortensen, and M. L. Sage, J. Chem. Phys. **100**, 6228 (1994).
[95] U. G. Jorgensen and P. Jensen, J. Mol. Spectrosc. **161**, 219 (1993); P. Jensen, J. Mol. Spectrosc. **133**, 438 (1989).
[96] Additional cc-pVTZ CCSD(T) results reveal that the relativistic correction varies substantially over the H_2O surface and has a different sign upon bending vs stretching. Some {relative energy, relativistic shift} data, in cm^{-1}, at selected [r(O–H) (Å), r(O–H′) (Å), ∠(H–O–H′) (deg)] points are: {0, 0} at [0.9588, 0.9588, 104.34]; {14 726, −47} at [1.1985, 1.1985, 104.34]; {37 206, −60} at [1.4382, 1.4382, 104.34]; {12124, +61} at [0.9588, 0.9588, 180]; {11768, +57} at [0.934, 0.934, 180]; and {202, +5} at [0.955, 0.955, 110.0]. In stretching the bonds symmetrically to the $O(^3P)+2H$ limit, the H_2O lone pairs transform toward doubly occupied $2s$ and $2p$ atomic orbitals in oxygen, thus gaining net s character, consistent with the observed negative sign of the relativistic shift. Rationalizing such data by considering only the rehybridization of the lone pairs certainly overlooks intricacies and risks oversimplification, but it appears to be of interpretive merit.
[97] O. L. Polyansky and J. Tennyson (personal communication).
[98] A succinct review of all aspects of the HNCO problem appears in Ref. 62. Very recent work on the photodissociation dynamics and bond-selective chemistry of this molecule has appeared in Ref. 99.
[99] W. Yi and R. Bersohn, Chem. Phys. Lett. **206**, 365 (1993); F. F. Crim, Annu. Rev. Phys. Chem. **44**, 397 (1993); S. S. Brown, H. L. Berghout, and F. F. Crim, J. Chem. Phys. **102**, 8440 (1995); J. Phys. Chem. **100**, 7948 (1996); J. Chem. Phys. **106**, 5805 (1997).
[100] G. O. Neely, J. Mol. Spectrosc. **27**, 177 (1968).
[101] A. D. McLean, G. H. Loew, and D. S. Berkowitz, J. Mol. Spectrosc. **72**, 430 (1978); C. Glidewell and C. Thomson, J. Mol. Struct.: THEOCHEM **104**, 287 (1983).
[102] M. Niedenhoff, K. M. T. Yamada, G. Winnewisser, and S. C. Ross, J. Mol. Struct. **352**, 423 (1995).
[103] J. D. Kemp and K. S. Pitzer, J. Am. Chem. Soc. **59**, 276 (1937); G. B. Kistiakowsky, J. R. Lacher, and F. Stitt, J. Chem. Phys. **7**, 289 (1939).
[104] K. S. Pitzer, Discuss. Faraday Soc. **10**, 66 (1951), and references therein.
[105] R. M. Pitzer and W. N. Lipscomb, J. Chem. Phys. **39**, 1995 (1963).
[106] R. F. W. Bader, J. R. Cheeseman, K. E. Laidig, K. B. Wiberg, and C. Breneman, J. Am. Chem. Soc. **112**, 6530 (1990).
[107] W. G. Fateley and F. A. Miller, Spectrochim. Acta **17**, 857 (1961); **19**, 611 (1963).
[108] S. Weiss and G. E. Leroi, J. Chem. Phys. **48**, 962 (1968).
[109] N. Moazzen-Ahmadi, H. P. Gush, M. Halpren, H. Jagannath, A. Leung, and I. Ozier, J. Chem. Phys. **88**, 563 (1988).
[110] R. Fantoni, K. van Helvoort, W. Knippers, and J. Reuss, Chem. Phys. **110**, 1 (1986).
[111] J. M. Fernández-Sánchez, A. G. Valdenebro, and S. Montero, J. Chem. Phys. **91**, 3327 (1989).
[112] U. Dinur and A. T. Hagler, J. Comput. Chem. **11**, 1234 (1990).
[113] W. E. Blass, G. W. Halsey, J. Susskind, D. C. Reuter, and D. E. Jennings, J. Mol. Spectrosc. **141**, 334 (1990).
[114] For example, E. Clementi and D. R. Davis, J. Chem. Phys. **45**, 2593 (1966).
[115] A. G. Császár, J. Am. Chem. Soc. **114**, 9569 (1992).
[116] C.-H. Hu, M. Shen, and H. F. Schaefer, III, J. Am. Chem. Soc. **115**, 2923 (1993).
[117] A. G. Császár, J. Phys. Chem. **100**, 3541 (1996).
[118] W. H. Hocking, Z. Naturforsch. A **31**, 1113 (1976).
[119] E. Bjarnov and W. H. Hocking, Z. Naturforsch. A **33**, 610 (1978).
[120] R. W. Davis, A. G. Robiette, M. C. L. Gerry, E. Bjarnov, and G. Winnewisser, J. Mol. Spectrosc. **81**, 93 (1980); E. W. Willemot, D. Dangoisse, J. Bellet, *ibid.* **73**, 96 (1978); J. Bellet, A. Deldalle, C. Samson, G. Steenbeckeliers, and E. R. Wertheimer, J. Mol. Struct. **9**, 65 (1971).
[121] I. D. Reva, A. M. Plokhotnichenko, E. D. Radchenko, G. G. Sheina, and Yu. P. Blagoi, Spectrochim. Acta A **50**, 1107 (1994).
[122] R. L. Redington, J. Mol. Spectrosc. **65**, 171 (1977).
[123] I. C. Hisatsune and J. Heicklein, Can. J. Spectrosc. **18**, 135 (1973).
[124] R. C. Millikan and K. S. Pitzer, J. Chem. Phys. **27**, 1305 (1957); T. Miyazawa and K. S. Pitzer, *ibid.* **30**, 1076 (1959).
[125] J. E. Bertie and K. H. Michaelian, J. Chem. Phys. **76**, 886 (1982), and references therein.
[126] N. L. Allinger, Z. S. Zhu, and K. Chen, J. Am. Chem. Soc. **114**, 6120 (1992).
[127] I. Yokoyama, Y. Miwa, and K. Machida, J. Am. Chem. Soc. **113**, 6458 (1991).
[128] K. B. Wiberg and K. E. Laidig, J. Am. Chem. Soc. **109**, 5935 (1987).
[129] G. I. L. Jonew and N. L. Owen, J. Mol. Struct. **18**, 1 (1973).
[130] A. J. Kirby, *The Anomeric Effect and Related Stereoelectronic Effects of Oxygen* (Springer-Verlag, Berlin, 1983).
[131] C. W. Bock, M. Trachtman, and P. George, J. Mol. Spectrosc. **84**, 256 (1980); G. A. Williams, J. N. Macdonald, and J. E. Boggs, J. Mol. Struct. **220**, 321 (1990); R. W. Williams and A. H. Lowrey, J. Comput. Chem. **12**, 761 (1991); L. Schäfer, C. Van Alsenoy, and N. Scarsdale, J. Mol. Struct.: THEOCHEM **86**, 349 (1982); T. K. Ha, R. Meyer, and H. H. Günthard, Chem. Phys. Lett. **59**, 17 (1978).
[132] C. W. Bock, P. George, and M. Trachtman, J. Mol. Spectrosc. **80**, 131 (1980).
[133] P. Ros, J. Chem. Phys. **49**, 4902 (1968); M. E. Schwartz, E. F. Hayes, and S. Rothenburg, *ibid.* **52**, 2011 (1970); A. C. Hopkinson, K. Yates, and I. G. Csizmadia, *ibid.* **52**, 1784 (1970); L. Radom, W. A. Lathan, W. J. Hehre, and J. A. Pople, Aust. J. Chem. **25**, 1601 (1972); B. V. Cheney and R. E. Christoffersen, J. Chem. Phys. **56**, 3503 (1972); M. R. Peterson and I. G. Csizmadia, J. Am. Chem. Soc. **101**, 1076 (1979); C. W. Bock, P. George, and M. Trachtman, J. Mol. Struct. **71**, 372 (1981); P. George, C. W. Bock, and A. Schmiedekamp, Chem. Phys. Lett. **80**, 127 (1981); C. Zirz and R. Ahlrichs, Theor. Chim. Acta **60**, 355 (1981); J. H. Van Lenthe, F. B. Van Duijneveldt, and M. M. M. Van Schaik, J. Mol. Struct. **88**, 333 (1982); A. D. McLean and Y. Ellinger, Chem. Phys. Lett. **98**, 450 (1983).
[134] T. Oie, I. A. Topol, and S. K. Burt, J. Phys. Chem. **99**, 905 (1995).
[135] A. St.-Amant, W. D. Cornell, P. A. Kollman, and T. A. Halgren, J. Comput. Chem. **16**, 1483 (1995).
[136] I. M. B. Nielsen, W. D. Allen, A. G. Császár, and H. F. Schaefer III, J. Chem. Phys. **107**, 1195 (1997).
[137] S. C. Ross, T. J. Butenhoff, E. A. Rohlfing, and C. M. Rohlfing, J. Chem. Phys. **100**, 4110 (1994).
[138] J. Olsen, O. Christiansen, H. Koch, and P. Jørgensen, J. Chem. Phys. **105**, 5082 (1996).